



Advanced technologies for molecular diagnosis of cancer: State of pre-clinical tumor-derived exosome liquid biopsies



Lin Li^{a,b}, Lili Zhang^{b,c}, Katelynn C. Montgomery^d, Li Jiang^a, Christopher J. Lyon^b, Tony Y. Hu^{b,d,*}

^a Department of Laboratory Medicine and Sichuan Provincial Key Laboratory for Human Disease Gene Study, Sichuan Academy of Medical Sciences & Sichuan Provincial People's Hospital, Chengdu, China

^b Center for Cellular and Molecular Diagnostics, Department of Biochemistry and Molecular Biology, School of Medicine, Tulane University, New Orleans, LA, USA

^c HCA Florida Healthcare Westside/Northwest Hospital Internal Medicine, Plantation, Florida, USA

^d Department of Biomedical Engineering, School of Science and Engineering, Tulane University, New Orleans, LA, USA

ARTICLE INFO

Keywords:

Cancer
Molecular diagnosis
Exosome
Isolation
Enrichment
Laboratory developed tests

ABSTRACT

Exosomes are membrane-defined extracellular vesicles (EVs) approximately 40–160 nm in diameter that are found in all body fluids including blood, urine, and saliva. They act as important vehicles for intercellular communication between both local and distant cells and can serve as circulating biomarkers for disease diagnosis and prognosis. Exosomes play a key role in tumor metastasis, are abundant in biofluids, and stabilize biomarkers they carry, and thus can improve cancer detection, treatment monitoring, and cancer staging/prognosis. Despite their clinical potential, lack of sensitive/specific biomarkers and sensitive isolation/enrichment and analytical technologies has posed a barrier to clinical translation of exosomes. This review presents a critical overview of technologies now being used to detect tumor-derived exosome (TDE) biomarkers in clinical specimens that have potential for clinical translation.

1. Introduction

Cancer is either the leading or second most common cause of death in most countries [1], partly due to lack of early diagnosis, since many cancers can be cured when detected and appropriately treated early in their development. Standard of care for the diagnosis and staging of solid tumors requires the surgical removal of a biopsy specimen that contains suspected tumor tissue and its subsequent analysis for cancer-associated factors (biomarkers or mutant alleles) or features (irregular cell shapes and sizes). A suspected tumor mass must be at least 2 mm in diameter for such analyses, to allow it to be identified by imaging modalities (e.g. magnetic resonance imaging or computed tomography) for directed sampling via a tissue biopsy [2]. However, such imaging modalities are susceptible to variability in identifications by radiologists and not all tumors can be biopsied safely due to risks associated with their anatomical location, a patient's performance status, and medications. Even when surgical biopsies are feasible, however, they still carry the risk of damage to adjacent tissue, infection, and the dissemination of cancer cells to other sites [3]. The urgent need for new methods to detect tumor

before they can be identified by imaging or surgically biopsied has led to the development of minimally invasive “liquid biopsies” (LBs) that permit molecular diagnosis of specific cancers using bio-fluids (e.g., blood, saliva, urine) that can be obtained using minimally or non-invasive procedures.

LB cancer tests approved by the Food and Drug Administration (FDA) analyze specific targets in the three best-characterized LB biomarker types: circulating tumor cells (CTCs), circulating tumor DNA (ctDNA), or cell-free RNA (cfRNA) released by apoptotic and necrotic tumor cells. The FDA has now approved several LB cancer tests, including four that detect ctDNA target sequences, five that detect cfDNA targets, and one CTC test [4]. The FDA has cleared five liquid biopsy tests for solid tumors in “general tumor profiling” or as “companion diagnostics” intended to aid clinicians in identifying patients who may benefit from targeted drug therapies [5].

While LB tests using CTCs, ctDNA, and cfRNA have demonstrated safety and efficacy, there are still biological and technological limitations that prevent their routine use by clinicians. Low LB concentrations of these analytes, especially early in disease progression, decrease test

* Corresponding author. Center for Cellular and Molecular Diagnostics, Department of Biochemistry and Molecular Biology, School of Medicine, Tulane University, New Orleans, LA, USA.

E-mail address: tonyhu@tulane.edu (T.Y. Hu).

<https://doi.org/10.1016/j.mtbio.2022.100538>

Received 19 October 2022; Received in revised form 27 December 2022; Accepted 28 December 2022

Available online 29 December 2022

2590-0064/© 2022 The Authors. Published by Elsevier Ltd. This is an open access article under the CC BY-NC-ND license (<http://creativecommons.org/licenses/by-nc-nd/4.0/>).

sensitivity and specificity. The presence of DNA and RNA from non-malignant cells in ctDNA and cfRNA sample can decrease diagnostic sensitivity and increase false negative rates, while the presence of DNA and RNA from non-malignant cells that carry cancer-associated mutations can decrease assay specificity and increase false positive rates. Both LB ctDNA and cfRNA are susceptible to degradation by circulating nucleases in the interval between LB collection and its processing for analysis or cryopreservation [6,7].

Extracellular vesicles (EVs), and particularly exosomes, have attracted increasing attention as the sources of cancer biomarkers since these vesicles are secreted at high concentration, particularly from diseased, injured, or malignant cells, and contain and preserve a wealth of biological information on their membranes and within their lumens. Numerous studies have demonstrated that EV-derived factors can serve as diagnostic biomarkers for different cancers. However, there are no FDA approved EV biomarker tests for cancer diagnosis to date, although an LB urine EV test for high-grade prostate cancer risk assessment has completed three clinical trials [8–10] and received an FDA “Breakthrough Device” designation as an important diagnostic technology [11].

Several reviews have discussed new tumor-derived exosome (TDE) assays [12–14], but this review differs from these as it covers recent research on TDE-LB assays that has progressed to analytical or clinical validation studies to evaluate their potential clinical utility and does not cover studies that did not use human LB samples or report the diagnostic power of their tests. This review focuses on studies that use advanced materials/methods to overcome challenges of conventional analytical

tools that have limited sensitivity for exosomes, including integrated platforms that use nanotechnology to enrich TDEs and detect TDE biomarkers on one device for rapid and accurate cancer diagnosis, and discusses considerations for improved clinical adoption of new TDE assays.

2. Exosome biogenesis and functional role in cancer

Cells secrete three major classes of EVs (exosomes, microvesicles, and apoptotic bodies) that differ by biogenesis and release pathways, size, composition and function. Exosomes are the smallest EVs (40–160 nm diameter), the only EVs that derive from the endosome pathway, are actively released by all cells, and can exhibit different composition under normal and stress conditions.

Exosome biogenesis initiates by inward budding of the early endosome membrane to generate a multivesicular body (MVB) that contains numerous intraluminal vesicles (ILVs) that are released into the extracellular space as mature exosomes upon fusion of the MVB and plasma membranes (Fig. 1). Exosomes contain material derived from the cytosol and the endosome membrane, which can contain factors derived from multiple organelles, and can thus reflect a cell's phenotype at the time of their secretion, although several processes can influence exosome composition and exosomes derived from the same cell can be heterogeneous in size, content, and function [15].

Exosomes play key roles in cell-to-cell communication by transferring regulatory molecules that can alter cell phenotypes (e.g., RNA/DNA,

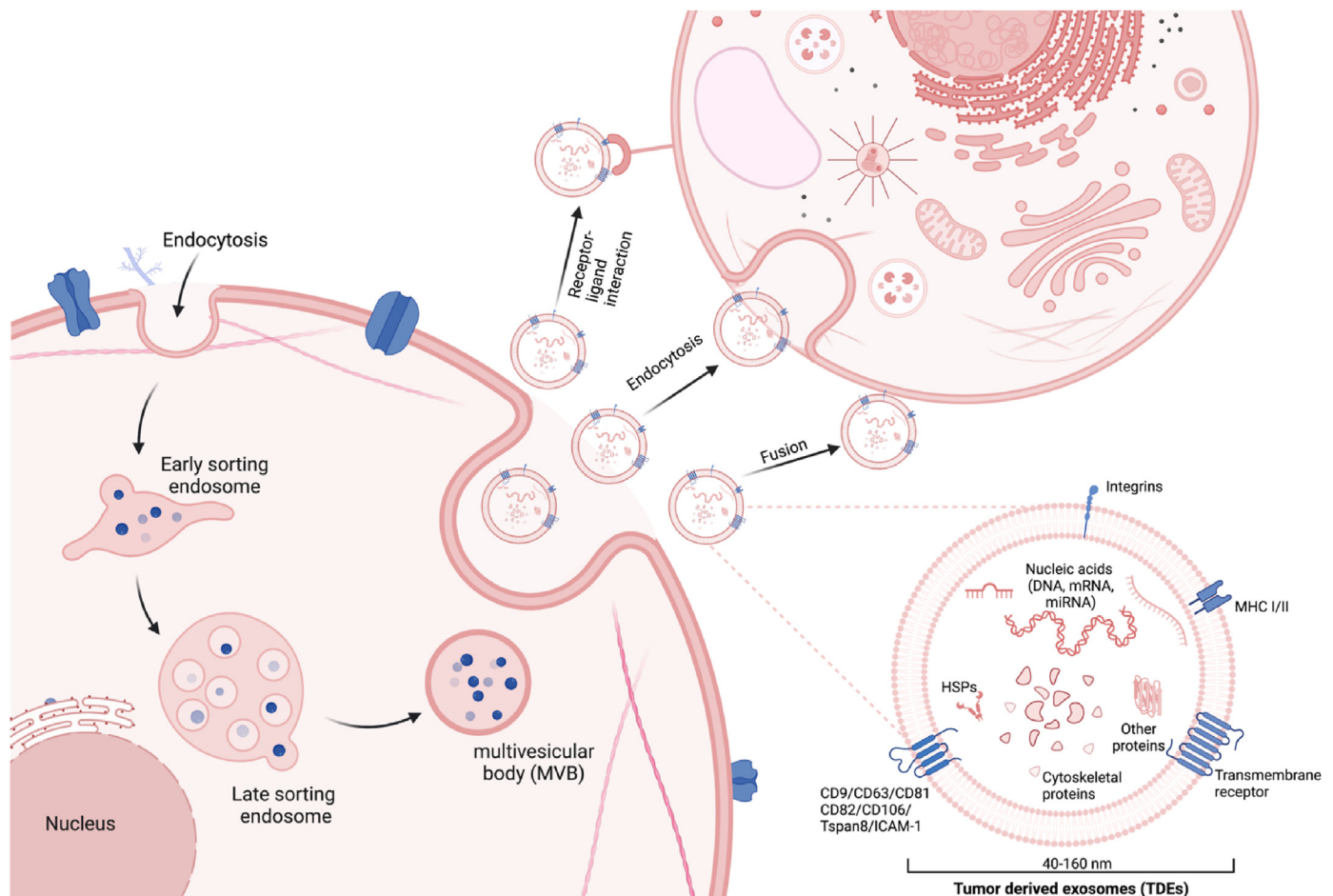


Fig. 1. EV biogenesis, secretion, uptake and composition. EV biogenesis initiates by the inward budding of the early endosome membrane to generate late multivesicular bodies that can secrete mature exosomes into the extracellular space. These EVs can incorporate a complex mixture of factors that derive from multiple cellular compartments. These include lipids, nucleic acids (DNA, mRNA, and miRNA), proteins, and other factors that can play important regulatory roles in cell-to-cell communication events when these factors are internalized by recipient cells following EV endocytosis, fusion or receptor-ligand interactions.

proteins, peptides, metabolites, and other factors) to recipient cells through endocytosis, membrane fusion, or ligand-receptor interactions [16–18]. This includes interactions that regulate tumor growth and metastasis since factors carried by TDEs can alter the behavior of cells in the tumor microenvironment and at distant sites to regulate the four major stages of tumor metastasis (invasion, intravasation, extravasation and colonization) (Fig. 2) [19–21]. For example, during the invasion stage of metastasis, Wnt2B-enriched TDEs facilitate cancer cell migration through extracellular matrix around the vascular endothelium by activating fibroblast proliferation [22] and remodeling the basement membrane to disrupt endothelial cell contacts [23]. TDEs also transfer factors (e.g., miR-1307–5p [24]) to cancer cells passing through the vascular endothelium (intravasation) to induce an epithelial-mesenchymal transition and an invasive mesenchymal phenotype in the resulting CTCs [25]. These CTCs can exit the circulation (extravasation) at pre-metastatic niches (PMNs) prepared by circulating TDEs released by primary tumors, and these sites can be cancer selective (e.g., TDE integrin $\beta 4$ and $\beta 5$ expression can respectively promote lung and liver PMNs) [23]. PMN colonization is regulated by TDEs that transfer miRNAs that promote the proliferation these micro-metastases (e.g., via miR-21, miR-204, miR-375 [26]) and the angiogenesis required to support tumor growth (e.g., via miR-148a, miR-21–5p) [25,27,28]. For example, vascular endothelial cell uptake of miR-210-enriched TDEs secreted by adjacent hepatocellular carcinoma cells can promote angiogenesis by inhibiting SMAD4 and STAT6 gene expression [29].

TDEs can also aid tumor cells in evading recognition and clearance by the immune system by reducing the abundance or attenuating the activity of cells with cytotoxic phenotypes. For example, TDEs can down-regulate NKG2D expression on natural killer cells to reduce their proliferation, migratory capacity, and cytotoxic activity [30]. TDE interactions with cytotoxic $CD8^+$ T cells can also induce their apoptosis through Fas/FasL or PD-L1/PD-1 interactions [31–33]. TDEs can also inhibit effector T cell proliferation and stimulate $CD4^+$ helper T cells to differentiate into regulatory T cells to attenuate pro-inflammatory immune reactions that can enhance tumor recognition and clearance by the

immune system. Similarly, TDEs can induce macrophages to adopt an anti-inflammatory M2-like tumor associated macrophage (TAM) phenotype and produce chemokines, cytokines, and enzymes that inhibit T cell effector function [34]. For further information on the role of TDEs in these processes, we recommend readers read reviews written by Wee et al. [23] and Whiteside et al. [35,36].

3. Tumor derived exosome biomarkers

As described above, TDEs are ideal candidates for cancer biomarkers since they can regulate multiple stages of tumor development and progression [37,38], including metastasis; are highly abundant in LB specimens; may carry biomarkers that permit their enrichment from biospecimens with complex EV compositions; and may carry several cancer-associated biomarkers to allow multiplex analyses with greater specificity. Notably, CTCs also protect their contents from extracellular hydrolases and allow simultaneous enrichment of multiple biomarkers but circulate at very low concentration and may reflect changes that occur after their escape from the primary tumor site [39]. Further, the only FDA-approved CTC application (CellSearch) is not a cancer diagnostic but an adjunct CTC enumeration assay that measures changes in CTC number to monitor or predict cancer progression, response to therapy, or to detect recurrent disease [4].

TDE biomarker discovery and new EV biosensing platform development and validation studies frequently employ cell culture supernatants [18,40], but clinical validity studies must be performed with highly complex human LB samples to ensure the test can separate and detect TDEs from other materials in the appropriate LB specimen type.

Numerous clinical validation studies that report diagnostic accuracy by area under the receiver operating characteristic curve (AUC) values have been performed for TDE biomarkers associated with different cancers using various LB specimen types and a variety of TDE biomarker selection strategies and isolation/detection approaches (Table 1). However, most analyses still employ RT-qPCR or ELISA to analyze TDEs from bulk isolation methods, including approaches that employ differences in

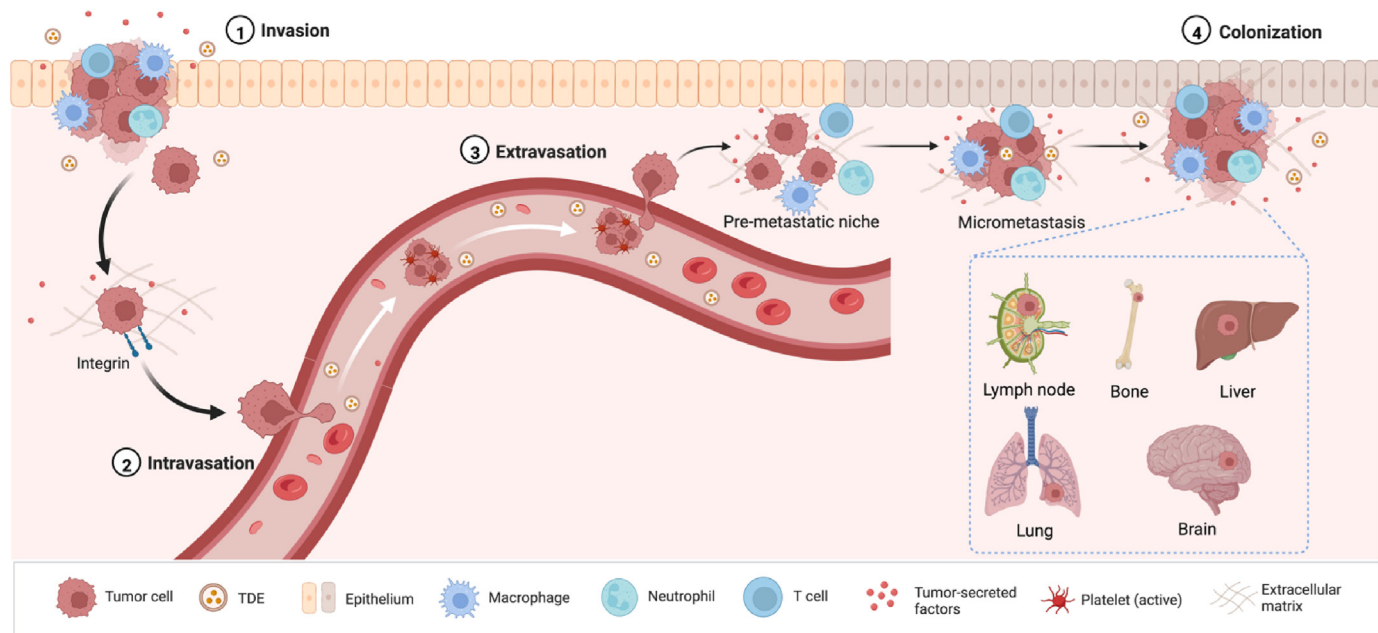


Fig. 2. Overview of the role of TDEs in the four steps of the metastatic cascade (invasion, intravasation, extravasation, and colonization). TDEs facilitate cancer cell invasion of neighboring tissue through disrupting the extracellular matrix by activating fibroblast proliferation. TDEs transfer factors to cancer cells to initiate an epithelial-mesenchymal transition to form circulating tumor cells (CTCs) during intravasation. These CTCs can then exit the circulation through the capillary bed (extravasation) at pre-metastatic niches (PMNs) prepared by the uptake of circulating TDEs released by the primary tumor. TDEs regulate the colonization of these PMNs by penetrating the vascular endothelium to transfer miRNAs that promote proliferation of micro-metastases and then angiogenesis required to support tumor growth.

Table 1
Summary of recently published studies on tumor-derived exosome liquid biopsies.

Cancer Type	Specimen ^a	Exosomal Biomarkers	Isolation/ Enrichment Methods ^b	Detection Methods	Diagnostic Accuracy (AUC) ^c	Clinical Applications ^d	Ref.
Bladder	Serum lncRNA	lnc-PCAT-1, lnc-UBC1, lnc-SNHG16	PP	RT-qPCR	Sum: 0.826	D,P	[47]
	Urine lncRNA	lnc-MALAT1, lnc- PCAT-1, lnc-SPRY4-1 T ¹	MA	RT-qPCR	Sum: 0.813	D,P	[48]
Breast	Plasma miRNA	let-7b-5p, miR- 122-5p, miR-146 b-5p miR-210-3p, miR- 215-5p	PP	RT-qPCR	Sum: 0.978	D	[49]
	Plasma miRNA	miR-150-5p miR-576-3p miR-4665-5p	PP	RT-qPCR	miR-150-5p: 0.705 miR-576-3p: 0.691 miR-4665-5p: 0.681	P	[50]
	Plasma MP	EGFR	UC	Microfluidic electrochemical immunosensor	EGFR: 0.903	D	[51]
	Plasma MP	CA 15-3, CA 125 CEA, HER2, EGFR, PSMA, VEGF, EpCAM,	TE	Fluorescence detection, machine learning	Sum: 0.9445	D,TM	[52]
	Plasma MP	EGFR, HER2, EpCAM	UC	Fluorescent aptasensor using aggregation-induced emission luminogens	Sum: 0.9845 EGFR: 0.9729 EpCAM: 0.6919 HER2: 0.5736	D,P	[53]
	Plasma MP	GPC-1	ImC	hMFEX/Fluorescence detection	GPC-1: 0.950	D,P	[54]
	Plasma mRNA	PGR, ESR1, ERBB2	UC	ddPCR, machine learning	Sum: 0.9302 PGR: 0.8670 ESR1: 0.8270 ERBB2: 0.7948	D,P	[55]
	Plasma miRNA	miR-1246, miR-221, miR-375, miR-21	MA	DNA probe: electrochemical biosensor using MDTs-CHA	Sum: 0.989 miR-1246: 0.931 miR-221: 0.942 miR-375: 0.958 miR-21: 0.947	D,P	[56]
	Serum miRNA	miR-375	UC	Thermophoretic amplification/ Nanoflare amplified fluorescence detection	miR-375: 0.960 miR-375 Stage I/II: 0.940	D,P	[57]
	Plasma MP	EpCAM, HER2	UC/IMC	SERS	EpCAM: 1.000 HER2: 1.000	D	[58]
Serum MP	EpCAM	ImC	Thermophoretic amplification/ fluorescence detection	EpCAM: 0.990	D,P	[59]	
Colorectal	Plasma	N/A	SEC	MALDI-TOF MS/Deep learning	Sum: 0.91	D	[60]
	Serum cRNA	I-circ-0004771	PP	RT-qPCR	Ihsa-circ-0004771: 0.860 hsa-circ-0004771 Stage I/II: 0.880	D	[28]
	Plasma MP	EGFR, EpCAM, CD24, GPA33	ImS	Electrochemical	Sum: 0.980	D,P	[61]
	Plasma MP Serum miRNA	EpCAM, CD63 miR-122	ImS PP	Single Molecule array RT-qPCR	Sum: 0.960 miR-122: 0.890	D,P D,P	[62] [63]
Endometrial	Plasma miRNA	miR-15a-5p	PP	ddPCR	miR-15a-5p: 0.813 miR-15a-5p + CEA + CA125: 0.899	D	[64]
Esophageal	Saliva chiRNA	GOLM1-NAA35	PP	RT-qPCR	GOLM1-NAA35: 0.912	D	[65]
Gastric	Serum miRNA	miR-92 b-3p, let-7g-5p miR-146 b-5p, miR-9- 5p	PP	RT-qPCR	miR-92 b-3p: 0.788 let-7g-5p: 0.850 miR-146 b-5p: 0.784 miR-9-5p: 0.920	D	[41]
	Serum piRNA/ miRNA	piR-019308, piR- 004918 piR-018569, miR- 1307-3p	MA	RT-qPCR	miR-1307-3p: 0.845 piR019308: 0.820 piR-004918: 0.754 piR-018569: 0.732 miR-1307-3p + CEA + CA: 0.902 piR019308 +CEA + CA: 0.914	D,P	[19]
	Serum lncRNA	HOTTIP	PP	RT-qPCR	HOTTIP: 0.827, HOTTIP + CEA + CA: 0.870	D,P	[66]
	Serum miRNA	miR-15 b-3p	MA	RT-qPCR	miR-15 b-3p: 0.820	D,P	[67]
	Plasma lncRNA	lnc-UEGC1	UC	qPCR	lnc-UEGC1: 0.876	D	[6]
HCC	Serum lncRNA	lnc-FAM72D-3, lnc- EPC1-4 lnc-85	UC	qPCR	FAM72D-3: 0.584 EPC1-4: 0.576	D,P	[68]
			Patented reagent	RT-qPCR	lnc85: 0.873	D	[69]

(continued on next page)

Table 1 (continued)

Cancer Type	Specimen ^a	Exosomal Biomarkers	Isolation/ Enrichment Methods ^b	Detection Methods	Diagnostic Accuracy (AUC) ^c	Clinical Applications ^d	Ref.
General	Plasma lncRNA						
	Serum miRNA	miR-224	PP	RT-qPCR	miR-224: 0.910	D,P	[70]
	Serum miRNA	miR-10 b-5p, miR- 215-5p	UC	RT-qPCR	miR-10 b-5p: 0.946 miR-215-5p: 0.701	D,P	[71]
	Serum miRNA	miR-122, miR-148a	PP	RT-qPCR	miR-122: 0.990	D,P	[72]
	Plasma miRNA	miR-1307-5p	PP	RT-qPCR	miR-1307-5p: 0.958	P	[24]
	Ascites MP	CD63, Cd24, EpCAM, MUC1	AuNP and gold growth	TPEX-chip - fluorescence	Colorectal Sum: 0.971 Gastric Sum: 0.938	D,P	[44]
	Serum MP	CD63 PTK7 EpCAM LZH8 HER2 PSA CA125	TE	Fluorescence linear discrimination analysis	SUM: 1.000 CD63: 0.9433 PTK7: 0.8097 EpCAM: 0.9163 LZH8: 0.8581 HER2: 0.8084 PSA: 0.7128 CA125: 0.8844	D,P	[73]
	Plasma MP	CD63 PD-L1	PP	ExoADM proximity bioassay- fluorescence detection	PD-L1_Prostate: 0.9850 PD-L1_NSCLC: 0.9889	D,T,P	[74]
	Serum MP	EGFR, CXCR4	ImC	Single EV - Flow Cytometry	EGFR: 0.900	D,P	[75]
	Serum cRNA	circHIPK3, circSMARCA5	SEC	ddPCR	circSMARCA5: 0.823 circHIPK3: 0.855 SUM + NLR + PLR + LMR: 0.901	D	[76]
HCC	Plasma miRNA	AFP, GPC3, ALB, APOH, FABP1 FGB, FGG, AHSG, RBP4, TF miR-92 b	Nanowires and covalent bonds	ddPCR	Sum: 0.870	D	[77]
Lung	Serum miRNA	miR-21	PP	RT-qPCR	miR-92 b: 0.925	D,ER	[78]
	Plasma miRNA	miR-21	Microfluid platform	RT-qPCR	Sun: 1.000	D, P, TM	[79]
	Plasma	N/A	SEC	SERS/Deep Learning	Stage I/II: 0.912 Stage I: 0.910 Stage 1 A: 0.844 SUM: 0.811 SLC9A3-AS1: 0.760 PCAT6: 0.705 BRAF: 0.720 PD-L1: 0.867	D,P	[80]
Melanoma	Blood lncRNA	SLC9A3-AS, PCAT6	MA	miDER-chip - dPCR	SUM: 0.811 SLC9A3-AS1: 0.760 PCAT6: 0.705 BRAF: 0.720 PD-L1: 0.867	D	[81]
NPC	Plasma DNA	BRAF	PP	dPCR	BRAF: 0.720	P, TM	[82]
	Plasma MP	PD-L1	UC	ELISA	PD-L1: 0.867	P, TM	[33]
NSCLC	Serum MP	Nucleolin, PD-L1	ImC	CRISPR - fluorescence	Early-stage: 0.905 Advanced-stage: 0.940	D,P	[83]
	Serum MP	CD109, EGFR	ImC	CRISPR- fluorescence	Sum: 0.934 CD109: 0.758 EGFR: 0.870	D,P	[84]
	Plasma MP	LPM1, EGFR	ImC	Gold nanoparticle-based proximity ligation assay	LPM1: 0.956, EGFR: 0.906	D	[55]
Ovarian	Serum miRNA	miR-9-3p, miR- 205-5p miR210-5p, miR- 1269a	PP	RT-qPCR	Sum: 0.878	D,P	[45]
	Plasma RNA/ DNA	EGFR	UFC	qPCR	Sum: 0.940	D	[46]
Ovarian	Serum MP	PD-L1	ImS	SERS	PD-L1: 0.970	D,P	[85]
	Plasma MP	CD24, FR α , EpCAM	3D nano-HB ImC	Nano-HB ELISA	CD24: 1.000 EpCAM: 1.000 FR α : 0.995 Sum: 0.709	D,P	[86]
	Plasma MP	EGFR, HER2, CA125, Fra CD24, EpCAM, CD9, CD63	ImC	Microplate ELISA	Sum: 1.000 CD24: 1.000 FR α : 1.000 EpCAM: 0.987 CA125: 0.987 EGFR: 0.853 HER2: 0.827 CD9/63: 0.733	D,P	[43]
	Serum miRNA	miR-375, miR-1307	PP	RT-qPCR	Sum: 0.837 Sum + CA125: 0.977	D,P	[87]
Ovarian	Plasma miRNA	miR-4732-5p	PP-PEG/DEX	RT-PCR	miR-4732-5p: 0.889	D	[88]
	Plasma MP	CD63, EpCAM, CD24	ImS	MV-Chip ELISA assay	CD24+EpCAM: 0.995 EpCAM: 0.985	D	[89]

(continued on next page)

Table 1 (continued)

Cancer Type	Specimen ^a	Exosomal Biomarkers	Isolation/ Enrichment Methods ^b	Detection Methods	Diagnostic Accuracy (AUC) ^c	Clinical Applications ^d	Ref.
Pancreatic	Serum miRNA	miR-145, miR-200c	PP	RT-qPCR	CD24: 0.928 CD63: 0.752 miR-145:0.910 miR-200c: 0.802	D	[90]
	Serum miRNA	miR-191, miR-21, miR-451a	PP	RT-qPCR	miR-21: 0.826 miR-191: 0.788 miR-451a: 0.759	D,P	[20]
	Serum miRNA Serum MP	miRNA-10 b EpCAM, EphA2	LmS-Lipid nanoprobe ImC	SERS Dye and quantum dot based fluorescent immunoassay	miRNA-10 b: 0.996 Sum: 0.770 DiO normalized Sum:0.950 EpCAM: 0.720 DiO normalized EpCAM: 0.920 EphA2: 0.750, DiO normalized EphA2: 0.930 SUM: 0.770 DiO normalized SUM: 0.950	D	[91] [92]
Prostate	Blood MP	GPC1, CD63	ACE-chip-electric and ImC	On-chip immunofluorescence	Sum: 0.989	D,P	[93]
	Serum MP	CD9, CD63, EGFR, MIF, GPC-1, EpCAM	ImC on PDA chip	PEARL SERS immunoassay	MIF: 0.886 GPC-1: 0.674 EGFR: 0.629 Sum: 0.700	D,RA	[94]
	Urine RNA	ERG, PCA3, SPDEF	UFC	RT-aPCR & proprietary test algorithm	Sum: 0.700	D,RA	[10]
	Serum MP	EphrinA2	UC	ELISA	EphrinA2: 0.766	D	[95]
	Serum miRNA	let-7a, let-7c, miR-200b, miR-141, miR-21	MA	AuTNP-laminated plasmonic biosensor	Sum: 1.000	D	[96]
	Serum miRNA Serum MP	miR-1246 PSMA, EpCAM	PP TE	Digital Nanostring nCounter Fluorescence detection	miR-1246: 0.926 Sum: 0.95	D,P D	[97] [98]

^a MP: Membrane protein; cRNA: circulation RNA.

^b UC: Ultracentrifugation; UFC: Ultra-filtration centrifugation; PP: Polymer precipitation; MA: Membrane affinity; ImC: Immunocapture; ImS: Immunomagnetic separation; LmS: Lipid mediated-separation; TE: Thermophoretic enrichment; SEC: Size-exclusion chromatography.

^c AUC: area under the receiver operating characteristic curve, where AUC = 0.5 denotes no classification ability and AUC = 1 denotes perfect classification.

^d D: Diagnosis;P: Prognosis; ER: Early recurrence; TM: Treatment monitoring; RA: Risk assessment; SP: Subtype prediction.

exosome density (e.g., ultracentrifugation) or surface charge (e.g., polymer coprecipitation) to separate them from other LB components. However, novel approaches, including microfluidic platforms, have shown that it is possible to integrate the isolation, enrichment, and detection of TDEs from small LB volumes. This includes diagnostic tests that analyze individual or combinations of TDE protein or nucleic acid biomarkers. TDE biomarker panels tend to exhibit greater diagnostic accuracy than single biomarker tests [41–44] as do multifactor tests that combine TDE miRNA or piRNA results with serum biomarker results [41, 45] or TDE RNA or DNA biomarker results with cDNA results [46].

4. Advances in EV isolation from liquid biopsies

Some exosome isolation methods that are useful for research applications are not suitable for use in clinics, as they require specialized equipment, trained personnel, and are labor intensive (Table 2). Ultracentrifugation is a gold-standard approach for exosome isolation in research laboratories but uses expensive equipment (\$50–100 K capital cost and \$3 K/year running costs), is slow (>4 h), and produces exosome samples with low and variable yields (5%–25% recovery) [99]. Commercially available polymer-based exosome precipitation kits (e.g., ExoQuickTM) do not require expensive equipment but have low

Table 2

Advantages and disadvantages of EV enrichment and detection method.

Methods	Advantages	Disadvantages	
EV isolation/ enrichment	Ultracentrifugation	High purity, large and small sample volumes	Expensive equipment, time-consuming, low and variable recovery
	Polymer precipitation	Simple procedure, high recovery	Low specificity, time-consuming
	Size-exclusion chromatography	High reproducibility, simple procedure	Low specificity
	Ultrafiltration	Label-free, easy preparation	Low specificity
	Affinity enrichment	High specificity	Antibody costs
	Thermophoretic enrichment	Cost-effective, simple procedure	Low specificity
EV detection	Electroacoustic enrichment	Label-free, contactless	Low specificity
	Digital PCR	Reproducibility, absolute quantification, high sensitivity	Limited multiplex capacity
	Electrochemical	Rapid, point-of-care potential, cost-effective, simple procedure	Low specificity
	Surface plasmon resonance	Label-free, real-time, high sensitivity, high throughput	Non-specific binding
	Surface-enhanced Raman scattering	High enhancement factor, stable, no quenching and photobleaching, fingerprint characteristics and narrow Raman bands	Spectra are complex and nonconforming
CRISPR	High sensitivity	Limited multiplex ability	

specificity, some versions require overnight incubation times (>12 h), and may have statements indicating that they are expressly not designed, intended, or warranted for use in humans or for therapeutic or diagnostic use [100]. Affinity-based EV enrichment methods permit high specificity EV isolation without expensive equipment but may exhibit reduced yield and primarily use antibodies for EV capture and enrichment, which can add significant cost to EV isolation. Cost reduction approaches for such affinity enrichment methods have thus focused on using aptamers for EV capture, since aptamers are easier and less expensive to synthesize and modify at scale than antibodies. Thermophoretic EV enrichment is faster and less expensive than affinity-based EV isolation methods, but is designed for microscale samples due to the constraints of the isolation method and is thus usually directly coupled to a method to detect a specific EV biomarker. Microfluidic electroacoustic enrichment is also cost-effective, and can isolate EVs directly from biological samples at high yield and purity, but is also not for large scale EV isolation due to its low flow rate. Further, standard thermophoretic and electroacoustic EV enrichment approaches are not capable of isolating TDEs from other EVs.

Exosome isolation remains an essential first step in validating the clinical specificity of exosome biomarkers, and new isolation methods should ideally increase exosome purity and yield and reduce isolation costs and operator time (Fig. 3). Several studies have thus investigated new approaches that directly capture TDEs from biospecimens without a coupled analysis step.

4.1. EV affinity enrichment

There has been a shift from bulk EV isolation via biophysical characteristics to small-scale EV isolation by affinity capture using antibodies and aptamers to surface proteins [44,99,101,102]. EVs can be directly captured from complex biological samples by antibodies to tetraspanin proteins (CD9, CD63, CD81) expressed on most EVs, and then analyzed with a tumor-specific affinity probes [92]. Most of these methods employ affinity-modified surfaces or beads (agarose or magnetic) [10] for EV capture, simplifying EV wash steps and providing large contact areas to improve capture efficiency to increase purity and lower sample volumes requirement [99]. New approaches have attempted to improve the

efficiency of immunoaffinity EV capture by increasing their available surface area (e.g., using microfluidic chips with 3D herringbone nanopatterns) [86]. These methods provide can have high specificity without requiring expensive equipment, but can still have high per test costs due to their use of EV capture antibodies. Cost reduction approaches for these methods have primarily focused on employing aptamers rather than antibodies for biomarker-specific EV capture since aptamers are easier and less expensive to modify and synthesize at scale than antibodies [22]. However, one group has used a surface modification approach that deposits material around EVs interacting with magnetic nanoparticles to generate a surface with impressions matching the dimensions of these EVs to promote efficient EV capture in the absence of affinity reagents [89]. This study reported that these reusable “magnetic colloid antibody” nanoparticles permitted rapid, low-cost isolations of EVs through the recognition of their size and shape, producing higher EV yields in 20 min than that achieve after a 4 h ultracentrifugation procedure.

EVs can also be directly captured from clinical samples by affinity separation strategies that utilize the special lipid properties of EV surface membranes. $\text{Fe}_3\text{O}_4/\text{TiO}_2$ nanoparticles (NPs) have been used for EV affinity enrichment as their TiO_2 outer shell interacts with EV phospholipids to allow magnetic capture of $\text{Fe}_3\text{O}_4/\text{TiO}_2$ NP/EV complexes and the subsequent analysis of a target miRNA [91] or surface protein [85] with an Au@Ag@MBA Surface Enhanced Raman Scattering (SERS) tag signal. Similarly, another group has reported that magnetic NPs conjugated with the phosphatidylserine receptor Tim4 perform better for EV enrichment than those conjugated with anti-CD63 or anti-CD9 antibodies [103]. Off-target interactions with lipid micelles, lipoproteins, and other lipid-rich particles can reduce the performance of lipid-affinity EV capture methods, but a templated plasmonic for exosomes (TPEX) platform proposes to address this by simultaneously evaluating the biophysical and biomolecular composition of the same vesicles [44]. In this approach, a sample is incubated with fluorescent TDE-specific aptamers and gold nanoparticles (AuNP), so that the formation of a gold nanoshell on vesicles with the exosome size range (40–160 nm diameters) quenches bound aptamers to increase accuracy by eliminating signal from other vesicles, non-vesicles, and free protein. This approach was validated using ascites samples to diagnose colorectal and gastric cancer (Table 1).

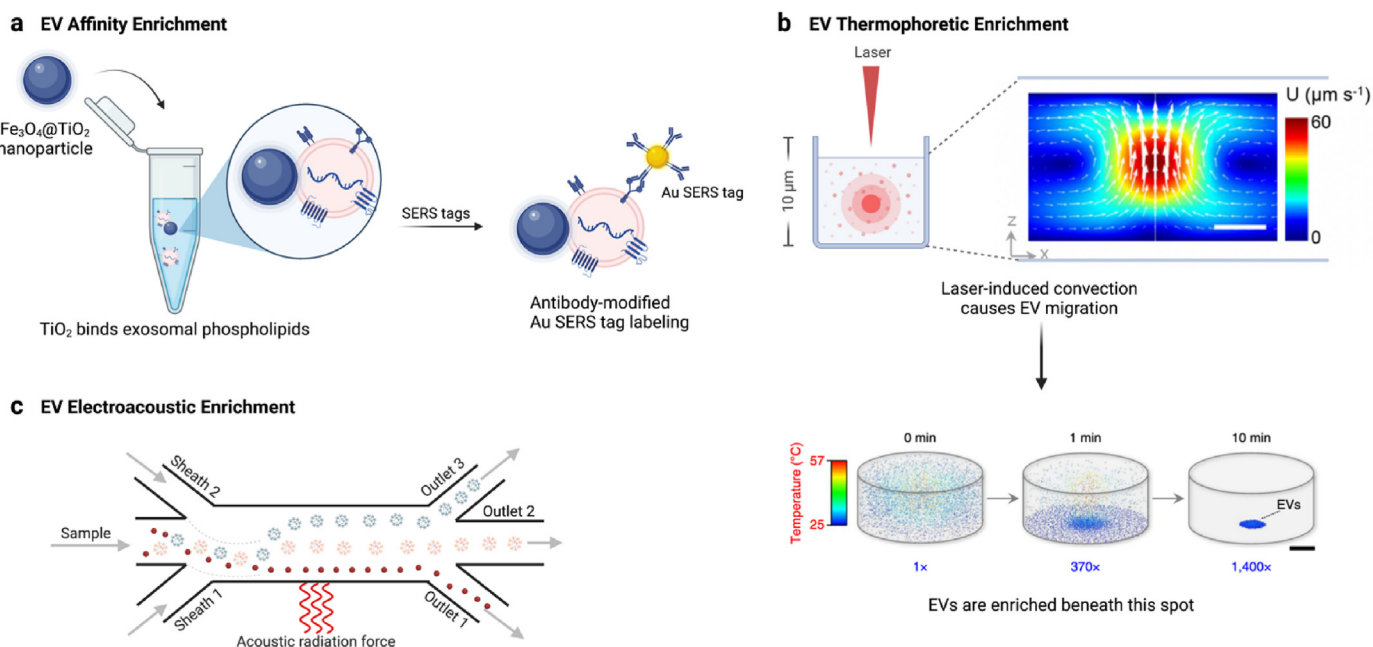


Fig. 3. New methods for EV isolation from liquid biopsies. (a) Affinity enrichment: $\text{Fe}_3\text{O}_4/\text{TiO}_2$ nanoparticles binding of EV membrane phospholipids for EV enrichment prior to miRNA or protein analysis; (b) Thermophoretic enrichment: laser irradiation forms a region of localized convection that concentrates EVs at the cold lower surface of the microfluidic chamber. (c) Electroacoustic enrichment: electroacoustic energy focused on a biospecimen exerts differential force on its contents based on their size and density to allow EVs to be separated from other components during passage across a microfluidic chamber.

4.2. EV thermophoretic enrichment

Non-affinity enrichment approaches have also been developed that employ physical properties to enrich EVs from other biospecimen components. This includes thermophoretic enrichment, which employs an induced temperature gradient to induce small particles in solution to move within a temperature gradient according to their intrinsic properties. One thermophoretic aptasensor (TAS) approach employed an infrared laser to heat a localized region of diluted serum sample to produce a temperature gradient and detected localized enrichment of EVs labeled with a fluorescently-tagged aptamer probe. In this method, the movement of aptamer-tagged EVs (30–1000 nm) was dominated by thermophoresis, causing them to move downward to the cool end of the assay microchamber, while convection dominated the overall movement of the unbound aptamer EV probe and small proteins (hydrodynamic diameters of only a few nm) to prevent their localized enrichment [73]. A more recent study has employed polyethylene glycol to attenuate diffusion during thermophoretic EV enrichment and fluorescence resonance energy transfer (FRET) to detect EVs that bind two TDE-specific biomarker probes to develop an assay that can detect prostate cancer-derived EVs in serum within 15 min to discriminate individuals with prostate cancer and benign prostate hyperplasia with 91% accuracy [98]. Another study established a “thermophoretic sensor implemented with nanoflares” (TSN) platform to detect EVs containing a specific miRNA target without requiring an RNA extraction or target amplification step. This TSN approach employed gold nanoflares consisting of small gold NPs conjugated with an antisense ssDNA oligonucleotide to the assay's target miRNA and hybridized to a fluorescently tagged short complementary oligonucleotide. EVs that internalize these nanoflares and express the target miRNA can displace this fluorescent oligonucleotide to remove the proximity-induced attenuation of its signal by the gold NPs, allowing thermophoretic EV signal enrichment to be detected by fluorescence microscopy [57]. These TAS and TSN approaches are faster and less expensive than antibody-mediated EV capture and detection methods, and have been applied to detect a biomarkers associated with several different cancers (TAS) or a breast cancer-associated biomarker (TSN) in serum (Table 1).

4.3. EV electroacoustic enrichment

Electroacoustic based methods can continuously separate small volume samples with less structural damage and sample loss than other methods, making this a promising approach for exosome separation [104]. One group has employed ultrasound to exert differential acoustic force to isolate exosomes from human blood products based on their size and density with a 90% isolation yield [105]. Similarly, a second group developed a platform that integrated acoustics and microfluidics to isolate exosome directly from whole blood, first using microscale cell-removal modules to remove 99.9% of large blood components (RBCs, WBCs and platelets) and then isolating exosomes at 98.4% purity [106]. This group subsequently reported that this approach could be used to isolated exosomes from saliva, where it generated exosome yields that were 15-fold higher than the gold standard of differential centrifugation [107]. A third group developed a device that used two coupled oscillators to generate dual-frequency transverse waves on an ultrafiltration membrane to prevent fouling effects and allow rapid label-free isolation of high yield and purity exosomes from LB specimens [108]. However, while these acoustofluidic platforms are cost-effective, they have limited ability to differentiate TDEs from other EVs.

5. Advances in TDE nucleic acid and protein detection

Exosome carry proteins, small RNAs, genomic DNA that can indicate the phenotype of their parental cells or regulate the behavior of their recipient cells (e.g., activate or suppress immune responses, tumor growth and cancer metastasis) allowing them to serve as candidate

biomarkers for tumor diagnosis, prognosis, and disease recurrence. TDE nucleic acids can play important roles in cancer diagnosis, as indicated by one study that found that the detection rate for activating EGFR mutations in a non-small cell lung cancer cohort using TDE nucleic acid versus ctDNA was 98% versus 82%, and this difference was even more pronounced (74% versus 26%) in patients with intrathoracic disease, indicating a substantial benefit for early diagnosis [109].

5.1. Digital PCR detection

RNAs comprise most of the exosome nucleic acid cargo [102] but are present a low concentration and thus are often enriched and purified from isolated EV samples before their analysis by a sensitive and specific detection approach, with or without a pre-amplification step. Reverse-transcription quantitative polymerase chain reaction (RT-qPCR) assays are a well-established, inexpensive, and high throughput means to quantify specific RNA targets [7,64,110,111] but have shown variable performance when applied to measure scarce RNA targets. Recent refinements employ water-oil emulsion technology [64,77] (digital droplet PCR; ddPCR) or microchamber platforms [81] (digital chamber PCR; dcPCR) to partition analysis samples into millions of picoliter volumes that are amplified and then read separately as individual reactions. This increases sensitivity and accuracy of the PCR readouts by measuring the percentage of positive droplets [110]. Notably, unlike PCR, ddPCR and dcPCR tests do not require a standard curve or reference sample, have high tolerance for biological inhibitors in samples, and can detect rare targets by decreasing signal competition [76]. Further, multiple EV miRNA biomarkers linked to malignant disease, including glioma, hepatocellular carcinoma (HCC), endometrial, and breast cancers, have been detected and validated in LB specimens by ddPCR (Table 1).

5.2. Electrochemical detection

Electrochemical approaches for EV detection often capture EVs on a functionalized electrode surface and measure changes in electrochemical signals that reflect changes in the number of bound EVs [112]. However, electrochemical sensors have also been employed to identify EVs bearing specific biomarker. An electrochemical biosensor conjugated with a CD9 antibody was used to directly capture exosomes and subsequently detect ovarian cancer-specific TDEs that bound a CA125-specific antibody probe (Fig. 4A) [113]. Another study developed a sandwich-type electrochemical biosensing platform in which spiky Au@Fe₃O₄ nanoparticles conjugated with an aptamer specific for the cancer biomarker MUC1 were employed to capture EVs from biological samples so that EpCAM-mediated capture of these EV-nanoparticle complexes could efficiently reduce a graphene oxide/Prussian blue electrochemical to detect breast cancer exosomes with a LOD of 80 particles/μL (Fig. 4B) [114]. Another group has developed a high-throughput integrated magneto-electrochemical extracellular vesicle (HiMEX) to permit EV enrichment and molecular profiling from blood samples in less than an hour without a separate EV isolation step [61]. HiMEX signal is produced by biomarker-specific antibodies functionalized with enzymes that catalyze electrochemical reactions detected by an electrode array on the bottom of the 96-well HiMEX assay plate. The HiMEX assay LOD was estimated to be 1000-fold lower than ELISA, and HiMEX accurately diagnosed colorectal cancer by detecting a CRC-associated EV biomarker pattern in analyzed plasma samples [61] (Fig. 4C, Table 1).

DNA can also be programmed to form nanomaterials with specific structures due to its highly predictable base pairing properties, readily modified to impart new biochemical properties on these structures, and used as electrochemical sensor. Several distinct DNA nanomaterial geometries have been produced to date, but a tetrahedral DNA framework generated from four ssDNAs has recently gained popularity since it assumes a rigid structure can be readily functionalized at its vertices or on its edges to introduce specific properties at specific 3D positions. One group proposed a method to detect exosome miRNA by a multifunctional

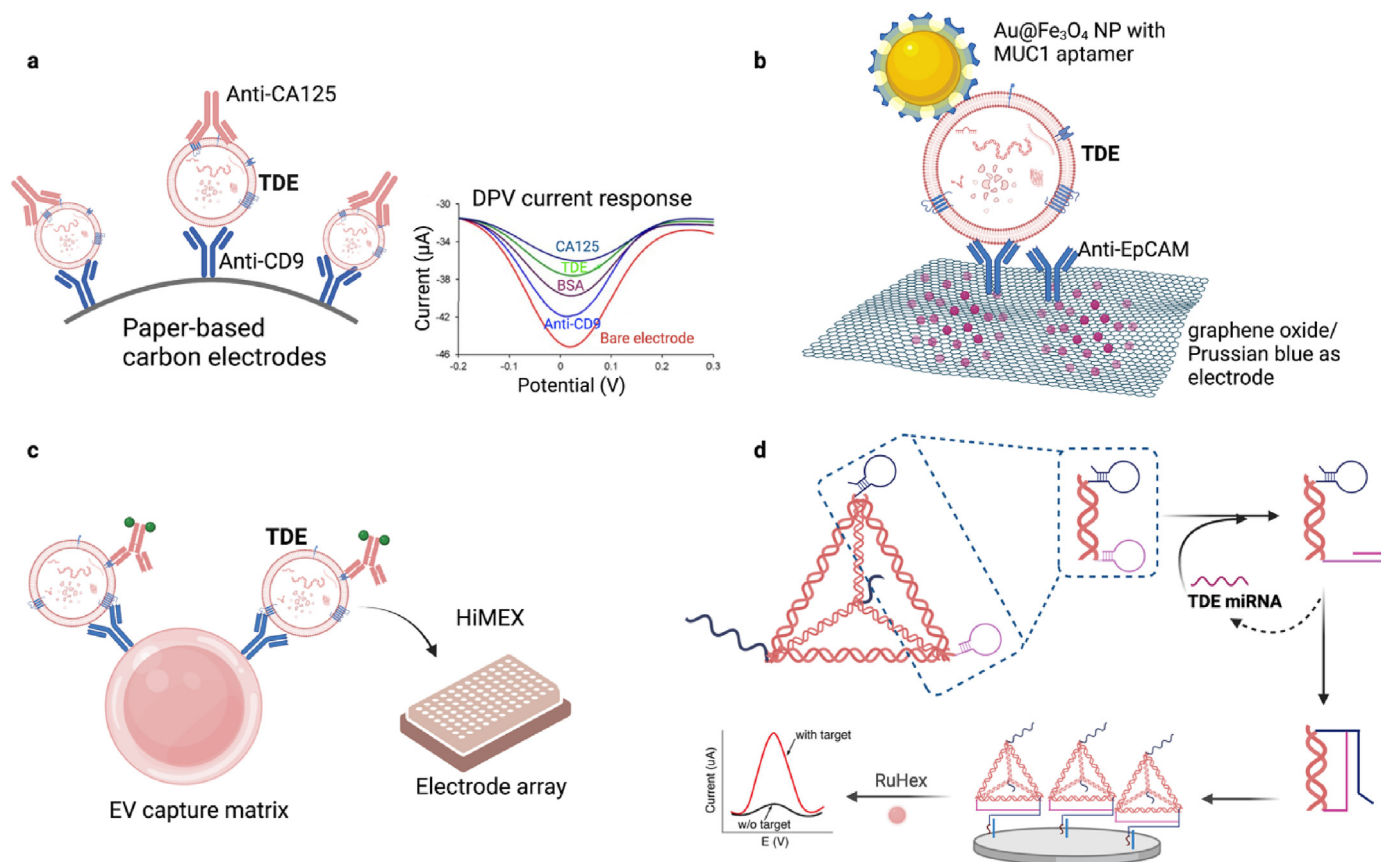


Fig. 4. Schematic representation of typical electrochemical platforms for TDE detection. (a) TDEs are captured by anti-CD9 antibodies conjugated to paper-based carbon electrodes (PCEs) and then hybridized with an antibody to a cancer biomarker (e.g., CA125), with differential pulse voltammetry (DPV) signal depicting the stepwise attachment of each layer on the PCEs surface. (b) Signal from TDEs captured by spiky Au@Fe₃O₄ nanoparticles conjugated with an MUC1 aptamer upon their capture on a graphene oxide/Prussian blue electrochemical probe by an EpCAM antibody. (c) TDEs enriched on antibody conjugated magnetic beads are magnetically immobilized on HiMEX electrode arrays that detect electrochemical reactions catalyzed by the enzyme-labeled antibodies detection antibodies bound to these TDEs. (d) Binding of a target miRNA to one of the two hairpins on a multifunctional DNA tetrahedron assisted catalytic hairpin assembly (MDTs-CHA) causes this hairpin to unfold and form a stable complex with the second hairpin and free a sequence that can then bind a capture probe on the surface of a detection electrode, after which incubation of bound MDTs-CHA RuHex produces a signal increase that is proportional to the concentration of the target miRNA.

DNA tetrahedron assisted catalytic hairpin assembly (MDTs-CHA) [56]. In this assay, specific and transient binding of the target miRNA to one of the two MDT hairpins causes it to unfold and form a stable complex with the second MDT hairpin (Fig. 4D). This produces an unpaired region that can then bind a capture probe on the surface of a detection electrode. These MDTs also contain a stable area for the binding of electroactive molecules and incubation of bound MDTs with RuHex produces an increase in signal that is proportional to the concentration of the target miRNA. This approach employs a rapid and simple procedure that does not require equipment and can detect exosome miRNA concentrations ≥ 7.2 aM within 30 min with high specificity and reproducibility. Furthermore, an assay that analyzed four exosome miRNAs (miR-21, -221, -375, and -1246) by this approach employed high diagnostic sensitivities for breast cancer and early breast cancer diagnosis (90.5% and 80%).

5.3. Surface plasmon resonance and surface-enhanced Raman scattering detection

Surface plasmon resonance (SPR) and surface-enhanced Raman scattering (SERS) assays can avoid the need to employ specific probes for biomarker detection and have been validated with plasma samples for the detection of breast and lung cancer in preliminary studies (Table 1). Both methods require significant technical expertise during assay development, as well as expensive equipment, but can provide

advantages versus other methods (Table 2).

SPR occurs when the absorption of an incident light coherent light source by electrons in a thin metal film causes free electrons to oscillate and produce a shift in the angle of the reflected versus the absorbed and emitted light, which can be altered by changes in the mass of biomolecules that are absorbed to this metal surface (Fig. 5A). SPR can thus be used to sensitively detect the binding of unlabeled target biomolecules by conjugating factors with affinity for these biomolecule targets on SPR sensors, since target binding decreases the intensity of the reflected beam and alters the SPR reflection intensity curve [96]. This approach has been employed for sensitive and specific detection of HER2-positive exosomes using a target-induced molecular aptamer beacon which upon binding to an exosome biomarker (HER2) exposes a guanine-rich tetramer region to bind hemin and catalyze the deposition of tyramine-coated gold nanoparticles on the exosome surface to markedly enhance their SPR signal (Fig. 5B) [115]. Another group used a biotinylated PD-L1 aptamer to capture PD-L1 + EVs on an SPR biosensor to permit label-free detection of exosome PD-L1 expression for real-time monitoring of tumor progression during immunotherapy (Fig. 5C) [116].

Surface-enhanced Raman scattering (SERS) analyses offer the potential to detect multiple EV biomarkers within the same sample volume (Fig. 6). This can be important since most TDE biomarker research studies analyze a single biomarker target, and thus ignore factors that have not been previously identified as important. However, it is also possible to analyze the molecular pattern or “fingerprint” of a TDE

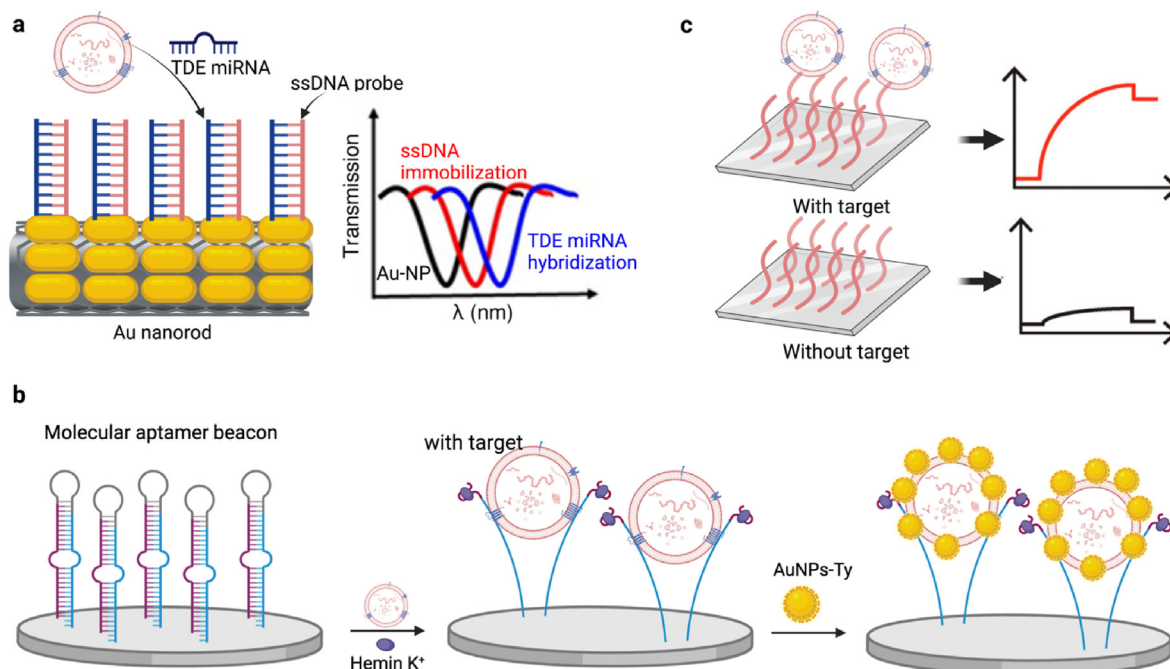


Fig. 5. Schematic for the application of surface plasmon resonance (SPR) to the measurement of EV concentration. (a) Binding of a TDE miRNA to a tapered optical fiber laminated with Au nanoparticles and functionalized with single strand DNA (ssDNA) specific for this miRNA causes a shift in the transmission spectrum proportional to target binding; (b) TDE binding to a molecular aptamer beacon conjugated to an SPR sensor exposes a guanine-rich tetramer region causing it to bind hemin and catalyze the deposition of tyramine-coated gold nanoparticles on the exosome surface to markedly enhance SPR signal; (c) Binding of a biotinylated aptamer to a TDE biomarker permits TDE capture and detection on an avidin conjugated SPR biosensor to permit label-free TDE detection.

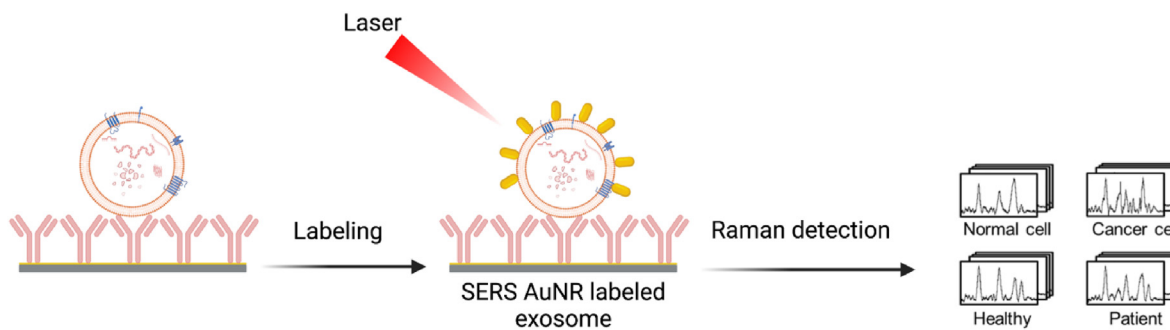


Fig. 6. Schematic for the application of surface enhanced Raman spectroscopy (SERS) to quantify EV concentration. EVs are first captured from a specimen by specific binding to target antibodies conjugated on the surface of the slide and then scanned to generate Raman spectra that are analyzed to detected TDE-specific SERS signatures.

without identifying its individual components [22]. SERS has significant potential for such studies, since it can produce narrow peak widths for analytes present at very low concentrations, and these factors can exhibit unique and distinct photon scattering signals. However, this requires that such assays be able to detect a specific biomarker-associated Raman scattering signature within the spectra produced by the entire sample. Two groups have employed deep learning to generate model that can distinguish SERS signal produced by plasma/serum EVs from patients with early-stage lung adenocarcinomas (stage IA, IB and IIB) or breast cancer (triple negative, HER2+, luminal A and B) versus their corresponding non-malignant controls to provide proof-of-principle data for the potential utility of this approach [80,117]. However, another study employed a Raman dye to produce a consistent SERS signal for EVs that were specifically captured by specific antibodies for targeted EV biomarker proteins. In this approach, SERS was employed to detect multiple analytes in the same assay by employing SERS to analyze a sensor slide conjugated with a microarray of antibodies to different EV proteins. In this assay, the abundance of EVs bound at each site on the

antibody array was determined by the SERS signal produced when nanorods (positively charged) loaded with the Raman reporter QSY21 were captured by electrostatic interaction with the membrane (negatively charged) of the captured EVs [58]. Both these assays required an EV pre-isolation step but this was offset by their ability to distinguish TDEs without having previously established a specific biomarker profile, or to enhance efficiency/throughput by analyzing the signal for multiple specific factors in a microarray format.

5.4. CRISPR/Cas-assisted detection

TDE biomarker proteins may be present a very low abundance and thus be difficult to detect by conventional methods that do not employ additional signal amplification methods. CRISPR signal amplification methods are one means to address this issue. For example, one group has recently employed an assay approach where aptamer binding induces a hybridization chain reaction (HCR) that stimulates CRISPR-Cas12a cleavage activity to enhance EV biomarker detection for the diagnosis

of nasopharyngeal carcinoma (Table 1) [83]. In this apta-HCR-CRISPR approach, aptamer binding to its EV protein target (nucleolin) induces a structural change that opens an aptamer sequence region (H0) that can hybridize with a hairpin sequence (H1) that binds a second hairpin sequence (H2) to initiate a hybridization cascade between these two hairpin sequences through toehold-mediated strand displacement. The H1 and H2 sequences are present at high concentration in this system, and their hybridization cascade produce long H1–H2 concatemers that are bound by a CRISPR-Cas12a/guide RNA (gRNA) complex specific for the repeated H1/H2 sequence element. This binding event induces the *trans* cleavage activity of the CRISPR-Cas12a/gRNA complex to cleave an abundant quenched fluorescent probe to produce a fluorescent signal proportional to the biomarker concentration (Fig. 7). CRISPR-based sensors have previously been employed to detect nucleic acids, small molecules, ions, but few EV proteins. The approach exhibited a limit of detection (LOD; 10^2 particles/ μL) that was orders of magnitude lower than those detected by aptamer-HCR-ELISA ($10^{3.9}$ particles/ μL) or aptamer-ELISA (10^6 particles/ μL). A separate study that employed PCR to amplify a CRISPR/gRNA target sequence from an EV-bound aptamer specific for by a similar CRISPR-mediated signal amplification method reported a limit of detection of 10^2 particles/ μL or CD109+ EVs in an EV assay intended for nasopharyngeal cancer diagnosis (Table 1) [84]. However, one limitation of all these CRISPR-Cas12a assay approaches is that only a single target can be detected per assay reaction since currently available CRISPR-Cas12a variants do not exhibit the *trans* cleavage specificity required for multiplex assays where the CRISPR/gRNA complexes associated with each biomarker target would need to accurately cleave a reporter probe with a biomarker-specific sequence and fluorescent tag to correctly quantify each biomarker.

5.5. MALDI-TOF MS detection

Matrix-assisted laser desorption/ionization time-of-flight mass spectrometry (MALDI-TOF MS) has been widely used to identify specific protein fingerprints associated with pathological changes in various diseases upon analysis of body fluids or tissue samples. MALDI-TOF MS has been recently applied to analyze TDEs for rapid diagnosis of melanoma, breast cancer, pancreatic cancer, early-stage lung cancer, and osteosarcoma [60,118–120]. MALDI-TOF MS spectra and SERS data of plasma EVs were used to discriminate TDEs of osteosarcoma patients from EVs of healthy controls for more accurate diagnosis of osteosarcoma [119]. Nanoparticles can be integrated into such MALDI-TOF MS analyses to increase the transfer of laser energy to sample molecules to increase assay sensitivity, as shown in one study that profiled small molecules of lung cancer-derived exosomes to differentiate early-stage non-small cell lung cancer patients from healthy controls [120]. MALDI-TOF MS fingerprints of isolated plasma TDEs from breast and pancreatic cancer patients have also been employed to develop a deep learning algorithm that demonstrated 80.0% diagnostic accuracy [60].

6. Advances in integrated point-of-care technologies: Microfluidic-chips

EV analysis procedures often require expensive equipment, complicated workflows, or significant technical expertise to enable sensitive detection of scarce EV populations of clinical interest, but these factors can limit their translation as research or clinical applications. Combination enrichment/detection diagnostic tests such as lateral flow-based point-of-care (POC) assays were originally created for resource-limited

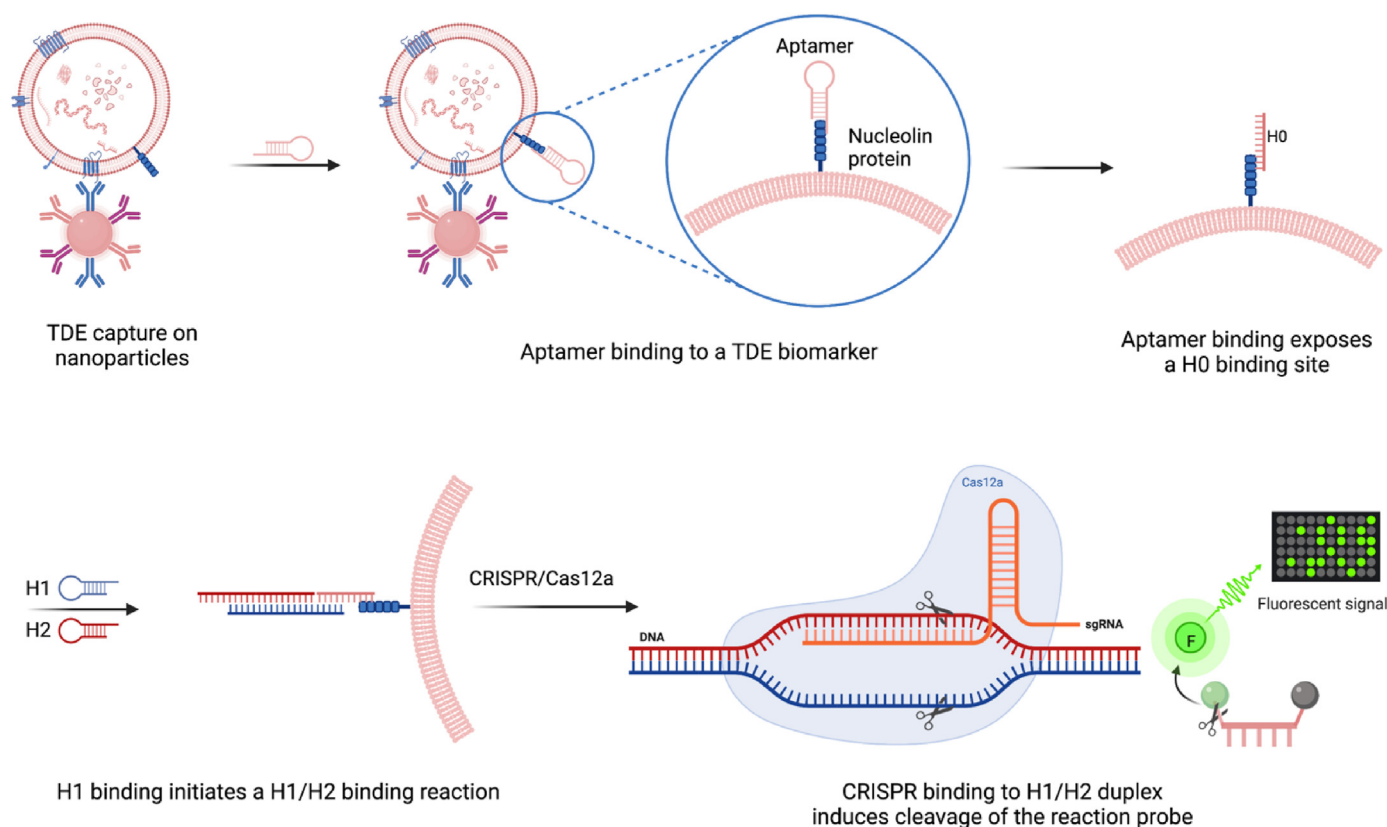


Fig. 7. Schematic of an apta-HCR-CRISPR dual amplification and Cas12a/fluorescent detection approach. In this method EVs are captured from a sample using nanoparticles coated with antibodies against an EV biomarker (CD63, CD81, CD9). Aptamer binding to a biomarker target (nucleolin) exposes a sequence that serves as a template for spontaneous assembly of two hairpin oligonucleotides (H1 and H2) present in excess to promote a hairpin chain reaction. These oligonucleotide concatemers are recognized by a CRISPR/Cas12a complex which then cleaves a quenched fluorescent probe in proportion to their abundance to indirectly quantify the abundance of the EV target molecule.

settings that may lack equipment or infrastructure required to perform sensitive or complex analyses. However, their low sample requirements, simple workflows, rapid results, and low costs make such POC assays attractive alternatives even well-equipped areas [121]. There has been significant growth in diagnostic POC technologies using microfluidics and engineered nanomaterials in last half decade, which has allowed miniaturization of assay platforms that integrate sample enrichment and biomarker detection workflows into a single procedure or sequential processes on an assay device. Employing such POC technologies on EV assays can assist analyze EV-associated biomarkers without isolating EVs from the input clinical specimen.

6.1. Electrochemical concentration and detection chip

EV biomarker analyses can be performed on POC devices that do not employ an EV isolation step when it is not necessary to isolate a target EV population to distinguish its signal from that contributed by other sources. For example, one study developed an integrated sample-to-answer microchip platform to directly measure an EV miRNA target in small plasma aliquots (Fig. 8) [79]. In this platform, surface acoustic waves produced by a generator on the lysis chip refract through a microfluidic channel to produce shear forces that lyse plasma EVs as they transit the chip to a concentrator/sensor chip. In this second chip, an applied voltage is used to concentrate the released EV nucleic acids and allow the target miRNA to hybridize with an anion exchange membrane conjugated with a complementary oligonucleotide. After miRNA hybridization, the initial current-voltage orientation is reversed to measure the captured miRNA concentration, which directly correlates with the voltage shift across the anion exchange membrane. The EV-derived contribution to this value is determined by repeating this process without the lysis step and subtracting this value from the value determined using the plasma lysate sample, which revealed a two order of magnitude enrichment of a target miRNA (miR-21) in the EV versus non-EV plasma miRNA fractions. This approach was reported to detect its target miRNA at 1 pM concentration in 20 μ L samples within 30 min and detected a >10-fold difference in the EV miR-21 expression level in plasma samples of liver cancer patients than healthy controls, although a formal diagnostic evaluation study was not performed using this method (Table 1).

6.2. Multiplexed immunocapture/fluorescence chip

Numerous groups have employed microfluidic chips to detect biomarkers present on the surface of EVs captured directly from biological samples, but these approaches often exhibit limitations associated with

mass transfer, surface interactions, and boundary effects. The incorporation of nanofeatures into such chip designs can alleviate many of these issues. For example, one group employed a multiscale integration by designed self-assembly (MINDS) approach to build porous 3D nanostructures to improve EV detection sensitivity by increasing the surface area available for affinity capture, enhancing the efficiency of sample mixing to improve surface interaction, and by decreasing boundary effects. ExoProfile chips fabricated with this 3D porous nano structure revealed an \sim 10-fold increase in binding capacity versus an equivalent chip design fabricated with a flat microchannel surface when both were conjugated with an EV capture antibody. This multiplex assay design employed a single channel approach for EV capture and then used parallel channels to capture and detect EVs bearing distinct surface biomarkers, where fluid flow is controlled by a pneumatic control layer (Fig. 9). This chip exhibited a 75% capture efficiency, a 4% channel-to-channel coefficient of variation, a four-log dynamic range, and a limit of detection of \sim 21 EV/ μ L when purified EVs captured on the chip were detected using an on-chip ELISA. Subsequent analysis of 10 μ L plasma aliquots from 15 patients with ovarian cancer and 5 benign controls on chips where each of the seven EV detection channels was loaded with capture antibodies to one of six ovarian cancer biomarkers and an EV detection antibody or no capture antibody, was found to accurately detect and classify the relative disease stage (I/II versus III/IV) of these patients (Table 1) [43].

7. Translational opportunities and challenges: clinical validation and user adoption

7.1. Regulations

Clinical diagnostics must obtain regulatory approval and meet analytical validation criteria, but do not always require clinical validation studies if they are employed as physician-prescribed Laboratory developed tests (LDTs) conducted in a Clinical Laboratory Improvement Amendment (CLIA)-certified laboratory. The Centers for Medicare and Medicaid Services (CMS) conducts laboratory inspections and analyzes the performance characteristics of such tests, including their accuracy, precision, analytical sensitivity, analytical specificity, reportable range, and reference intervals under the Public Health Services Act through CLIA. Once a lab is CLIA certified for a test, the test can only be performed at that location, with laboratory requiring its own certification. Once a LDT is FDA approved, it is referred to as an *in-vitro* diagnostic device (IVD) and no longer falls under the CMS but is instead covered by the Food, Drug, and cosmetic Act, as amended by the Medical Device Amendment of 1976 [122]. FDA approved IVDs can be legally marketed,

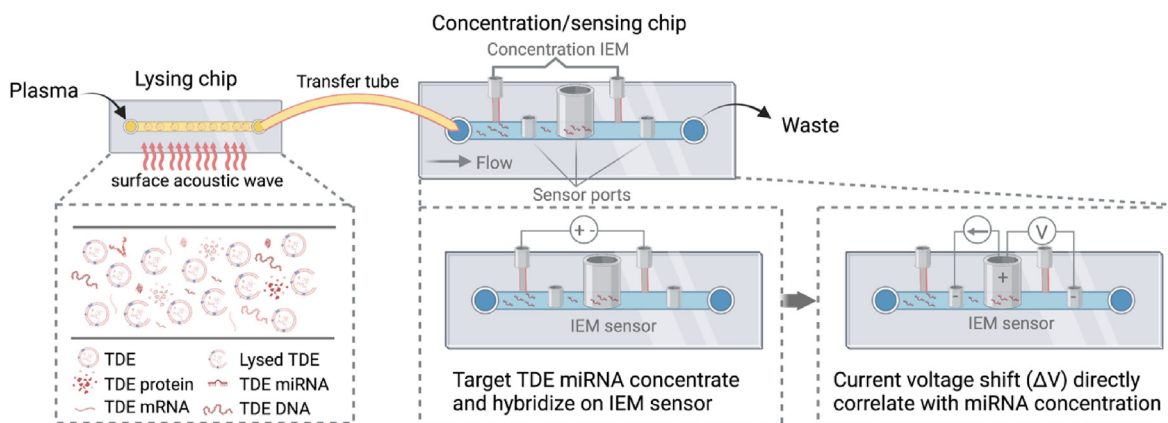


Fig. 8. Schematic of an integrated microfluidic platform for TDE-miRNA analysis. This device consists of a lysing chip in which plasma exosomes are lysed by a surface acoustic wave (SAW) after which miRNA from lysed TDEs is concentrated in a region upstream of a positively charged ion-exchange membrane (IEM) by an applied voltage. Following this concentration step, this miRNA is hybridized to a target-specific oligonucleotide conjugated to a negatively charged IEM and miRNA concentration is determined by the change in voltage produced by miRNA binding.

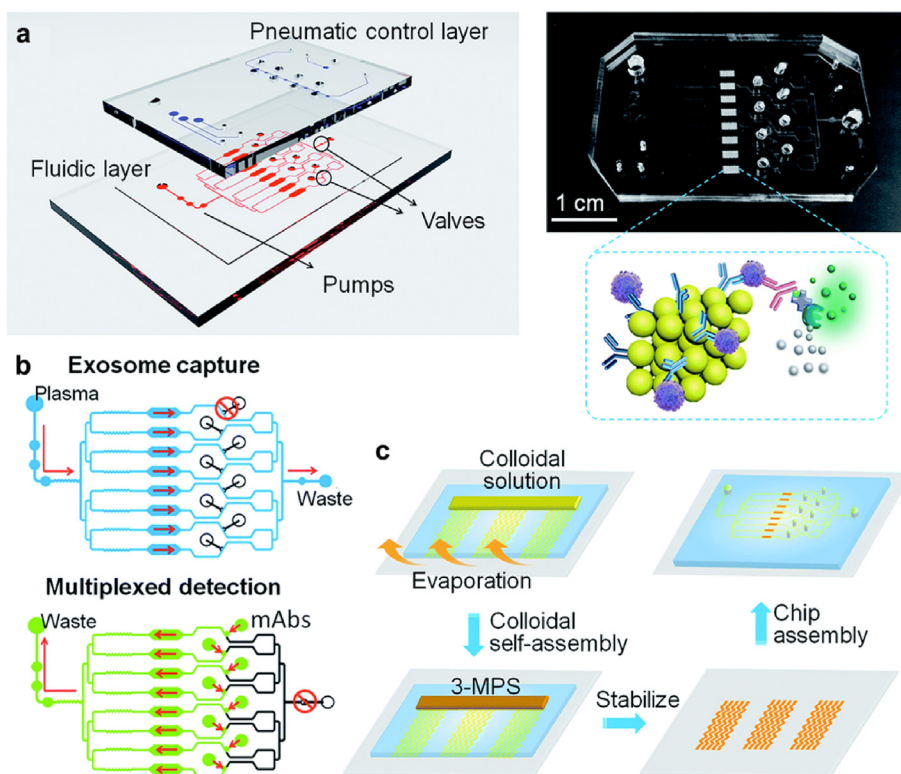


Fig. 9. Integrated exosome capture, isolation, and detection using the ExoProfile chip platform. (a) Schematic of the ExoProfile chip, which consists of a pneumatic and a fluidic layer and 3D serpentine nanostructures used for *in situ* exosome phenotyping; (b) Procedure for exosome immunocapture and multiplexed sample analysis, where EV samples are first loaded and captured the 3D nanostructures in the forward direction (blue) before the flow is reversed to (green) load monoclonal detection antibodies contained within the reagent reservoirs on the chip that are blocked during sample loading; (c) Workflow for chip fabrication by microfluidic colloidal self-assembly. Reprinted with permission from Zhang et al. 2019. Copyright 2019 The Royal Society of Chemistry.

sold, and used in any location without CLIA certifications.

FDA approval of an IVD indicates its analytical and clinical validity, and the FDA continues to monitor the IVD using post-market surveillance requirements and adverse event reporting to intervene if a problem needs to be rectified or if the device needs to be recalled from the market. There is no such oversight for LDTs, making FDA pre-market approval the gold standard for public safety. However, LDTs processed at CLIA certified labs have a role in the diagnostic market since an LDT might never file for IVD classification due to cost, infrequent use, instrument and/or interpretation requirements (mass spectrometry, flow cytometry, immunohistochemistry), or lack of desire to market outside of a laboratory or company. LDTs performed at CLIA certified labs can be safe and effective, as seen in recent years when the increase in patient needs and rapid access outnumbered the available supplies of IVDs, and the FDA relied on LDTs for COVID-19 detection [123].

7.2. Considerations for end user adoption

The ExoDx™ Prostrate (IntelliScore) Test developed by Exosome Diagnostics Inc. (acquired by Bio-Techne Corporation in 2018) has now shown clinical utility and been used by > 50,000 patients in their decision process, but success of the technology required defining a very specific problem and target population to address. The tests are only approved for “risk management” of men over 50 years of age with PSA level in the “grey zone” of 2–10 ng/mL [5]. The company listened to patients who wanted to avoid unnecessary biopsies and therefore cared more about a high negative predictive value than the overall performance of the test across all thresholds. The company worked with clinicians to determine a threshold value to maximize negative predictive value. The test can now predict high-grade prostate cancer with 91% negative predictive value. Testing is provided as a “medical service” and is reimbursed by insurance companies and government contracts the company has established. The LDT requires custom materials and equipment and is completed at a CLIA certified lab with a 4-day turnaround time from receiving the sample to sending results to the clinician.

In the meantime, Bio-Techne is working with the FDA for their PMA, which might change their business plan again when their IVD can be tested outside of their CLIA-certified labs. Researchers need to think about how a TDE-LB test is going to be used in the real-world and makes changes to their designs so they can be incorporated into the clinician's workflow and provide the information that align with the patients and clinicians goals.

8. Conclusion and future direction

New LB tests that analyze CTCs, cfDNA, or cRNA are gaining acceptance for diagnostic profiling and companion testing due to their safety and efficacy. Molecular diagnostics that analyze TDE biomarkers in LB samples should, however, provide even greater advantages since TDEs are abundantly secreted and accumulate in biofluids and carry and preserve factors that can regulate tumor remodeling and metastasis to provide a rich source of biomarkers that have potential for non-invasive early cancer diagnosis, phenotyping, treatment response evaluations.

This review discusses conventional and novel technologies used to isolate, enrich, detect, or analyze TDEs present in LBs or other complex biological samples. Recent studies have made impressive progress in increasing the performance of these methods using new approaches to improve TDE separation, cargo amplification, and analysis, including microfluidic devices that can streamline and integrate TDE isolation and analysis steps using nanostructure or nano-sensors. However, each of these approaches has its inherent strengths and weaknesses, and researchers must thus select the approach (es) that offer the best characteristics for their desired application and which can be integrated into a workflow suitable for a clinical laboratory or POC test [99]. Microfluidic platforms validated with complex biological samples, including LB specimens, have the potential to decrease time, costs, sample volumes required for EV biomarker tests, but clinical use of his technology has not been approved by the FDA and their use will require a full pre-market approval assessment.

EV study results can be influenced by methodological differences

between laboratories, which is why there is a push from groups like the EV-TRACK Consortium and International Society of Extracellular Vesicles (ISEV) to standardize sample handling (collection, processing, storage) and report transparent methods for EV isolation/enrichment and detection/quantification [124]. This is particularly important during the EV biomarker discovery phase since there are no standardized methods for EV isolation from cell culture or human body fluids, and different methods can yield EV populations with different compositions and purities that can confound independent validation studies.

The consistency of the EV population analyzed by an EV biomarker test is also critical for its reproducible diagnostic performance. No EV diagnostic tests have been approved by the FDA to date. LDTs performed at a certified laboratory using a standard protocol provide one means to address this issue, but integrated EV capture and analysis approaches similar to those described in this review could also provide a robust means of achieving reproducible assays results and could be applied in a variety of settings to enhance testing capacity.

Prior to their FDA approval and clinical adoption, EVs tests will need to demonstrate diagnostic power, safety, and efficacy. EV assays intended for early cancer detection will need to prove that early detection can have an impact on cancer survival. However, demonstrating this clinical utility can be challenging since even when random control intervention trials are performed to address this issue their results may be influenced by treatment decisions that may be only partly influenced by the EV test result [125]. Further, current TDE tests are not designed to indicate tumor location or extent, and thus may need to be used in conjunction with traditional diagnostic methods or as companion diagnostics, particularly when treatment requires tumor resection or radiation therapy rather than an anti-cancer drug regimen. Nonetheless, TDE assays have strong potential for early detection of cancers that are difficult to diagnose by conventional means, for precision medicine approaches with cancers that exhibit high mortality/poor prognoses, and for potential multi-cancer screening approaches.

RT-qPCR-based EV diagnostic assays are likely to be the first to reach clinical approval due to the prominence of EV RNA biomarkers in current TDE research studies and will likely rapidly proliferate since once the technology is proven safe and effective other diagnostic tests can apply for De Novo or 510 K applications with reduced regulatory hurdles. Such assays will likely employ biomarker panels to improve diagnostic power, and subsequent assay may employ different biomarker types (e.g., both soluble factors and TDE biomarkers) and deep learning or diagnostic algorithms to further enhance diagnostic power [80].

Credit author statement

Lin Li: Writing-original draft preparation; **Lili Zhang:** Writing-Review and Editing; **Katelynn C. Montgomery:** Writing-Review and Editing; **Li Jiang:** Writing-Review and Editing; **Christopher J. Lyon:** Writing-Review & Editing; **Tony Y. Hu:** Conceptualization, Writing-Review and Editing, Supervision, Project administration, Funding acquisition.

Declaration of competing interest

The authors declare that they have no known competing financial interests or personal relationships that could have appeared to influence the work reported in this paper.

Data availability

No data was used for the research described in the article.

Acknowledgements

The work was primarily supported by research funding provided by National Cancer Institute (U01CA252965), Eunice Kennedy Shriver

National Institute of Child Health and Human Development (R01HD090927, R01HD103511), National Institute of Allergy and Infectious Diseases (R01AI144168), U.S. Department of Defense (W81XWH1910926), National Institute of Neurological Disorders and Stroke (R21NS130542).

References

- [1] H. Sung, J. Ferlay, R.L. Siegel, M. Laversanne, I. Soerjomataram, A. Jemal, F. Bray, Global cancer statistics 2020: GLOBOCAN estimates of incidence and mortality worldwide for 36 cancers in 185 countries, *CA A Cancer J. Clin.* 71 (2021) 209–249, <https://doi.org/10.3322/caac.21660>.
- [2] D. Crosby, S. Bhatia, K.M. Brindle, L.M. Coussens, C. Dive, M. Emberton, S. Esener, R.C. Fitzgerald, S.S. Gambhir, P. Kuhn, T.R. Rebbeck, S. Balasubramanian, Early detection of cancer, *Science* 375 (2022), eaay9040, <https://doi.org/10.1126/science.aay9040>.
- [3] K. Shyamala, H.C. Girish, S. Murgod, Risk of tumor cell seeding through biopsy and aspiration cytology, *J. Int. Soc. Prev. Community Dent.* 4 (2014) 5–11, <https://doi.org/10.4103/2231-0762.129446>.
- [4] S. Gutman, Evaluation of Automatic Class III Designation CellSearch Epithelial Cell Kit/cell Spotter Analyzer, K031588, Center for Devices and Radiological Health (CDRH), 2004.
- [5] W. Yu, J. Hurley, D. Roberts, S.K. Chakraborty, D. Enderle, M. Noerholm, X.O. Breakefield, J.K. Skog, Exosome-based liquid biopsies in cancer: opportunities and challenges, *Ann. Oncol.* 32 (2021) 466–477, <https://doi.org/10.1016/j.annonc.2021.01.074>.
- [6] L.Y. Lin, L. Yang, Q. Zeng, L. Wang, M.L. Chen, Z.H. Zhao, G.D. Ye, Q.C. Luo, P.Y. Lv, Q.W. Guo, B.A. Li, J.C. Cai, W.Y. Cai, Tumor-originated exosomal lncUEG1 as a circulating biomarker for early-stage gastric cancer, *Mol. Cancer* 17 (2018) 84, <https://doi.org/10.1186/s12943-018-0834-9>.
- [7] M.V. Martínez-Domínguez, A. Zottel, N. Šamec, I. Jovčevska, C. Dincer, U.D. Kahlert, A.C. Nickel, Current technologies for RNA-directed liquid diagnostics, *Cancers* 13 (2021) 5060, <https://doi.org/10.3390/cancers13205060>.
- [8] A. Kretschmer, R. Tutrone, J. Alter, E. Berg, C. Fischer, S. Kumar, P. Torkler, V. Tadigotla, M. Donovan, G. Sant, J. Skog, M. Noerholm, Pre-diagnosis urine exosomal RNA (ExoDx EPI score) is associated with post-prostatectomy pathology outcome, *World J. Urol.* 40 (2022) 983–989, <https://doi.org/10.1007/s00345-022-03937-0>.
- [9] M.J. Donovan, M. Noerholm, S. Bentink, S. Belzer, J. Skog, V. O'Neill, J.S. Cochran, G.A. Brown, A molecular signature of PCA3 and ERG exosomal RNA from non-DRE urine is predictive of initial prostate biopsy result, *Prostate Cancer Prostatic Dis.* 18 (2015) 370–375, <https://doi.org/10.1038/pcan.2015.40>.
- [10] J. McKiernan, M.J. Donovan, E. Margolis, A. Partin, B. Carter, G. Brown, P. Torkler, M. Noerholm, J. Skog, N. Shore, G. Andriole, I. Thompson, P. Carroll, A prospective adaptive utility trial to validate performance of a novel urine exosome gene expression assay to predict high-grade prostate cancer in patients with prostate-specific antigen 2–10ng/ml at initial biopsy, *Eur. Urol.* 74 (2018) 731–738, <https://doi.org/10.1016/j.eururo.2018.08.019>.
- [11] Bio-Techne Corporation, FDA Grants Breakthrough Device Designation to Bio-Techne's ExoDx™ Prostate IntelliScore™ (EPI) Test, 2019. <https://www.prnewswire.com/news-releases/fda-grants-breakthrough-device-designation-to-bio-technes-exodx-prostate-intelliscore-epi-test-300868095.html>. (Accessed 15 June 2022). accessed.
- [12] X. Fang, Y. Wang, S. Wang, B. Liu, Nanomaterials assisted exosomes isolation and analysis towards liquid biopsy, *Mater. Today Bio.* 16 (2022), 100371, <https://doi.org/10.1016/j.mtbio.2022.100371>.
- [13] H. Cheng, Q. Yang, R. Wang, R. Luo, S. Zhu, M. Li, W. Li, C. Chen, Y. Zou, Z. Huang, T. Xie, S. Wang, H. Zhang, Q. Tian, Emerging advances of detection strategies for tumor-derived exosomes, *Int. J. Mol. Sci.* 23 (2022) 868, <https://doi.org/10.3390/ijms23020868>.
- [14] H. Xiong, Z. Huang, Z. Yang, Q. Lin, B. Yang, X. Fang, B. Liu, H. Chen, J. Kong, Recent progress in detection and profiling of cancer cell-derived exosomes, *Small* 17 (2021), e2007971, <https://doi.org/10.1002/sml.202007971>.
- [15] K. Valencia, L.M. Montuenga, Exosomes in liquid biopsy: the nanometric world in the pursuit of precision oncology, *Cancers* 13 (2021) 2147, <https://doi.org/10.3390/cancers13092147>.
- [16] S.E.L. Andaloussi, I. Mäger, X.O. Breakefield, M.J. Wood, Extracellular vesicles: biology and emerging therapeutic opportunities, *Nat. Rev. Drug Discov.* 12 (2013) 347–357, <https://doi.org/10.1038/nrd3978>.
- [17] C. Théry, K.W. Witwer, E. Aikawa, M.J. Alcaraz, J.D. Anderson, R. Andriantsitohaina, A. Antoniou, T. Arab, F. Archer, G.K. Atkin-Smith, D.C. Ayre, J.M. Bach, D. Bachurski, H. Baharvand, L. Balaj, S. Baldacchino, N.N. Bauer, A.A. Baxter, M. Bebawy, C. Beckham, A. Bedina Zavec, A. Benmoussa, A.C. Berardi, P. Bergese, E. Bielska, C. Blenkiron, S. Bobis-Wozowicz, E. Boilard, W. Boireau, A. Bongiovanni, F.E. Borràs, S. Bosch, C.M. Boulanger, X. Breakefield, A.M. Breglio, M. Brennan, D.R. Brigstock, A. Brisson, M.L. Broekman, J.F. Bromberg, P. Bryl-Górecka, S. Buch, A.H. Buck, D. Burger, S. Busatto, D. Buschmann, B. Bussolati, E.I. Buzás, J.B. Byrd, G. Camussi, D.R. Carter, S. Caruso, L.W. Chamley, Y.T. Chang, C. Chen, S. Chen, L. Cheng, A.R. Chin, A. Clayton, S.P. Clerici, A. Cocks, E. Cocucci, R.J. Coffey, A. Cordeiro-da-Silva, Y. Couch, F.A. Coumans, B. Coyle, R. Crescitelli, M.F. Criado, C. D'Souza-Schorey, S. Das, A. Datta Chaudhuri, P. de Candia, E.F. De Santana, O. De Wever, H.A. Del Portillo, T. Demaret, S. Deville, A. Devitt, B. Dhondt, D. Di Vizio, L.C. Dieterich, V. Dolo, A.P. Dominguez Rubio, M. Dominici, M.R. Dourado, T.A. Driedonks,

- F.V. Duarte, H.M. Duncan, R.M. Eichenberger, K. Ekström, S. El Andaloussi, C. Elie-Caille, U. Erdbrügger, J.M. Falcón-Pérez, F. Fatima, J.E. Fish, M. Flores-Bellver, A. Försonits, A. Frelat-Barrand, F. Fricke, G. Fuhrmann, S. Gabriellsson, A. Gámez-Valero, C. Gardiner, K. Gärtner, R. Gaudin, Y.S. Gho, B. Giebel, C. Gilbert, M. Gimona, I. Giusti, D.C. Goberdhan, A. Görgens, S.M. Gorski, D.W. Greening, J.C. Gross, A. Gualerzi, G.N. Gupta, D. Gustafson, A. Handberg, R.A. Haraszti, P. Harrison, H. Hegyesi, A. Hendrix, A.F. Hill, F.H. Hochberg, K.F. Hoffmann, B. Holder, H. Holthofer, B. Hosseinkhani, G. Hu, Y. Huang, V. Huber, S. Hunt, A.G. Ibrahim, T. Ikezu, J.M. Inal, M. Isin, A. Ivanova, H.K. Jackson, S. Jacobsen, S.M. Jay, M. Jayachandran, G. Jenster, L. Jiang, S.M. Johnson, J.C. Jones, A. Jong, T. Jovanovic-Taliman, S. Jung, R. Kalluri, S.I. Kano, S. Kaur, Y. Kawamura, E.T. Keller, D. Khamari, E. Khomyakova, A. Khvorova, P. Kierulff, K.P. Kim, T. Kislinger, M. Klingeborn, D.J. Klinke 2nd, M. Kornek, M.M. Kusanović, F. Kovács Á, E.M. Krämer-Albers, S. Krasemann, M. Krause, I.V. Kurochkin, G.D. Kusuma, S. Kuypers, S. Laitinen, S.M. Langevin, L.R. Languino, J. Lannigan, C. Lässer, L.C. Laurent, G. Lavie, E. Lázaro-Ibáñez, S. Le Lay, M.S. Lee, Y.X.F. Lee, D.S. Lemos, M. Lenassi, A. Leszczynska, I.T. Li, K. Liao, S.F. Libregts, E. Ligeti, R. Lim, S.K. Lim, A. Linē, K. Linnemannstöv, A. Llorente, C.A. Lombard, M.L. Lorenowicz, M. Lőrincz Á, J. Lötvall, J. Lovett, M.C. Lowry, X. Loyer, Q. Lu, B. Lukomska, T.R. Lunavat, S.L. Maas, H. Malhi, A. Marcilla, J. Mariani, J. Mariscal, E.S. Martens-Uzunova, L. Martin-Jaurar, M.C. Martínez, V.R. Martins, M. Mathieu, S. Mathivanan, M. Mauger, L.K. McGinnis, M.J. McVey, D.G. Meckes Jr., K.L. Meehan, I. Mertens, V.R. Minciocchi, A. Möller, M. Möller Jørgensen, A. Morales-Kastresana, J. Morhayim, F. Mullier, M. Muraca, L. Musante, V. Mussack, D.C. Muth, K.H. Myburgh, T. Najrana, M. Nawaz, I. Nazarenko, P. Nejsun, C. Neri, T. Neri, R. Nieuwland, L. Nimrichter, J.P. Nolan, E.N. Nolte-t Hoen, N. Noren Hooten, L. O'Driscoll, T. O'Grady, A. O'Loughlin, T. Ochiya, M. Olivier, A. Ortiz, L.A. Ortiz, X. Osteikoetxea, O. Østergaard, M. Ostrowski, J. Park, D.M. Pegtel, H. Peinado, F. Perut, M.W. Pfaffl, D.G. Phinney, B.C. Pieters, R.C. Pink, D.S. Pisetsky, E. Pogge von Strandmann, I. Polakovicova, I.K. Poon, B.H. Powell, I. Prada, L. Pulliam, P. Quesenberry, A. Radeghieri, R.L. Raffai, S. Raimondo, J. Rak, M.I. Ramirez, G. Raposo, M.S. Rayyan, N. Regev-Rudzki, F.L. Ricklefs, P.D. Robbins, D.D. Roberts, S.C. Rodrigues, E. Rohde, S. Rome, K.M. Rouschop, A. Rugghetti, A.E. Russell, P. Saá, S. Sahoo, E. Salas-Huenuleo, C. Sánchez, J.A. Saugstad, M.J. Saul, R.M. Schifferers, R. Schneider, T.H. Schøyen, A. Scott, E. Shahaj, S. Sharma, O. Shatnyeva, F. Shekari, G.V. Shelke, A.K. Shetty, K. Shiba, P.R. Siljander, A.M. Silva, A. Skowronek, O.L. Snyder 2nd, R.P. Soares, B.W. Sódar, C. Soekmadji, J. Sotillo, P.D. Stahl, W. Stoorvogel, S.L. Stott, E.F. Strasser, S. Swift, H. Tahara, M. Tewari, K. Timms, S. Tiwari, R. Tixeira, M. Tkach, W.S. Toh, R. Tomasini, A.C. Torrecilhas, J.P. Tosar, V. Toxavidis, L. Urbanelli, P. Vader, B.W. van Balkom, S.G. van der Grein, J. Van Deun, M.J. van Herwijnen, K. Van Keuren-Jensen, G. van Niel, M.E. van Royen, A.J. van Wijnen, M.H. Vasconcelos, L.J. Vechetti Jr., T.D. Veit, L.J. Vella, É. Velot, F.J. Verweij, B. Vestad, J.L. Viñas, T. Visnovitz, K.V. Vukman, J. Wahgren, D.C. Watson, M.H. Wauben, A. Weaver, J.P. Webber, V. Weber, A.M. Wehman, D.J. Weiss, J.A. Welsh, S. Wendt, A.M. Wheelock, Z. Wiener, L. Witte, J. Wolfram, A. Xagorari, P. Xander, J. Xu, X. Yan, M. Yáñez-Mó, H. Yin, Y. Yuana, V. Zappulli, J. Zarubova, V. Žekas, J.Y. Zhang, Z. Zhao, L. Zheng, A.R. Zheutlin, A.M. Zickler, P. Zimmermann, A.M. Zivkovic, D. Zocco, E.K. Zuba-Surma, Minimal information for studies of extracellular vesicles 2018 (MISEV2018): a position statement of the International Society for Extracellular Vesicles and update of the MISEV2014 guidelines, *J. Extracell. Vesicles* 7 (2018), 1535750, <https://doi.org/10.1080/20013078.2018.1535750>.
- [18] J. Tan, Y. Wen, M. Li, Emerging biosensing platforms for quantitative detection of exosomes as diagnostic biomarkers, *Coordination Chem. Rev.* 446 (2021), 214111, <https://doi.org/10.1016/j.ccr.2021.214111>.
- [19] L. Ge, N. Zhang, D. Li, Y. Wu, H. Wang, J. Wang, Circulating exosomal small RNAs are promising non-invasive diagnostic biomarkers for gastric cancer, *J. Cell Mol. Med.* 24 (2020) 14502–14513, <https://doi.org/10.1111/jcmm.16077>.
- [20] T. Goto, M. Fujiya, H. Konishi, J. Sasajima, S. Fujibayashi, A. Hayashi, T. Utsumi, H. Sato, T. Iwama, M. Ijiri, A. Sakatani, K. Tanaka, Y. Nomura, N. Ueno, S. Kashima, K. Moriichi, Y. Mizukami, Y. Kohgo, T. Okumura, An elevated expression of serum exosomal microRNA-191, -21, -451a of pancreatic neoplasm is considered to be efficient diagnostic marker, *BMC Cancer* 18 (2018) 116, <https://doi.org/10.1186/s12885-018-4006-5>.
- [21] L. Mashouri, H. Yousefi, A.R. Aref, A.M. Ahadi, F. Molaei, S.K. Alahari, Exosomes: composition, biogenesis, and mechanisms in cancer metastasis and drug resistance, *Mol. Cancer* 18 (2019) 75, <https://doi.org/10.1186/s12943-019-0991-5>.
- [22] L.J. Liang, Y. Yang, W.F. Wei, X.G. Wu, R.M. Yan, C.F. Zhou, X.J. Chen, S. Wu, W. Wang, L.S. Fan, Tumor-secreted exosomal Wnt2b activates fibroblasts to promote cervical cancer progression, *Oncogenesis* 10 (2021) 30, <https://doi.org/10.1038/s41389-021-00319-w>.
- [23] I. Wee, N. Syn, G. Sethi, B.C. Goh, L. Wang, Role of tumor-derived exosomes in cancer metastasis, *Biochim. Biophys. Acta, Rev. Cancer* 1871 (2019) 12–19, <https://doi.org/10.1016/j.bbcan.2018.10.004>.
- [24] J.W. Eun, C.W. Seo, G.O. Baek, M.G. Yoon, H.R. Ahn, J.A. Son, S. Sung, D.W. Kim, S.S. Kim, H.J. Cho, J.Y. Cheong, Circulating exosomal microRNA-1307-5p as a predictor for metastasis in patients with hepatocellular carcinoma, *Cancers* 12 (2020) 3819, <https://doi.org/10.3390/cancers12123819>.
- [25] C. Su, J. Zhang, Y. Yarden, L. Fu, The key roles of cancer stem cell-derived extracellular vesicles, *Signal Transduct. Targeted Ther.* 6 (2021) 109, <https://doi.org/10.1038/s41392-021-00499-2>.
- [26] D. Koppers-Lalic, M. Hackenberg, R. de Menezes, B. Misovic, M. Wachalska, A. Geldof, N. Zini, T. de Reijke, T. Wurdinger, A. Vis, J. van Moorselaar, M. Pegtel, I. Bijnsdorp, Non-invasive prostate cancer detection by measuring miRNA variants (isomiRs) in urine extracellular vesicles, *Oncotarget* 7 (2016) 22566–22578, <https://doi.org/10.18632/oncotarget.8124>.
- [27] L. Raimondi, A. De Luca, A. Gallo, V. Costa, G. Russelli, N. Cuscino, M. Manno, S. Raccosta, V. Carina, D. Bellavia, A. Conigliaro, R. Alessandro, M. Fini, P.G. Conaldi, G. Giavaresi, Osteosarcoma cell-derived exosomes affect tumor microenvironment by specific packaging of microRNAs, *Carcinogenesis* 41 (2020) 666–677, <https://doi.org/10.1093/carcin/bgz130>.
- [28] B. Pan, J. Qin, X. Liu, B. He, X. Wang, Y. Pan, H. Sun, T. Xu, M. Xu, X. Chen, X. Xu, K. Zeng, L. Sun, S. Wang, Identification of serum exosomal hsa-circ-0004771 as a novel diagnostic biomarker of colorectal cancer, *Front. Genet.* 10 (2019) 1096, <https://doi.org/10.3389/fgene.2019.01096>.
- [29] X.J. Lin, J.H. Fang, X.J. Yang, C. Zhang, Y. Yuan, L. Zheng, S.M. Zhuang, Hepatocellular carcinoma cell-secreted exosomal microRNA-210 promotes angiogenesis *in vitro* and *in vivo*, *Mol. Ther. Nucleic Acids* 11 (2018) 243–252, <https://doi.org/10.1016/j.omtn.2018.02.014>.
- [30] I.A. Batista, S.T. Quintas, S.A. Melo, The interplay of exosomes and NK cells in cancer biology, *Cancers* 13 (2021) 473, <https://doi.org/10.3390/cancers13030473>.
- [31] K.M. McAndrews, R. Kalluri, Mechanisms associated with biogenesis of exosomes in cancer, *Mol. Cancer* 18 (2019) 52, <https://doi.org/10.1186/s12943-019-0963-9>.
- [32] G. Chen, A.C. Huang, W. Zhang, G. Zhang, M. Wu, W. Xu, Z. Yu, J. Yang, B. Wang, H. Sun, H. Xia, Q. Man, W. Zhong, L.F. Antelo, B. Wu, X. Xiong, X. Liu, L. Guan, T. Li, S. Liu, R. Yang, Y. Lu, L. Dong, S. McGettigan, R. Somasundaram, R. Radhakrishnan, G. Mills, Y. Lu, J. Kim, Y.H. Chen, H. Dong, Y. Zhao, G.C. Karakousis, T.C. Mitchell, L.M. Schuchter, M. Herlyn, E.J. Wherry, X. Xu, W. Guo, Exosomal PD-L1 contributes to immunosuppression and is associated with anti-PD-1 response, *Nature* 560 (2018) 382–386, <https://doi.org/10.1038/s41586-018-0392-8>.
- [33] M. Cordonnier, C. Nardin, G. Chanteloup, V. Derangere, M.P. Algros, L. Arnould, C. Garrido, F. Aubin, J. Gobbo, Tracking the evolution of circulating exosomal-PD-L1 to monitor melanoma patients, *J. Extracell. Vesicles* 9 (2020), 1710899, <https://doi.org/10.1080/20013078.2019.1710899>.
- [34] Y. Chen, Y. Song, W. Du, L. Gong, H. Chang, Z. Zou, Tumor-associated macrophages: an accomplice in solid tumor progression, *J. Biomed. Sci.* 26 (2019) 78, <https://doi.org/10.1186/s12929-019-0568-z>.
- [35] T.L. Whiteside, Tumor-derived exosomes and their role in cancer progression, *Adv. Clin. Chem.* 74 (2016) 103–141, <https://doi.org/10.1016/bs.acc.2015.12.005>.
- [36] T.L. Whiteside, Exosomes carrying immunoinhibitory proteins and their role in cancer, *Clin. Exp. Immunol.* 189 (2017) 259–267, <https://doi.org/10.1111/cel.12974>.
- [37] G. Brock, E. Castellanos-Rizaldos, L. Hu, C. Coticchia, J. Skog, Liquid biopsy for cancer screening, patient stratification and monitoring, *Transl. Cancer Res.* 4 (2015) 280–290.
- [38] K. Hosseini, M. Ranjbar, A. Pirpour Tazehkand, P. Asgharian, S. Montazersaheb, V. Tarhiz, T. Ghasemnejad, Evaluation of exosomal non-coding RNAs in cancer using high-throughput sequencing, *J. Transl. Med.* 20 (2022) 30, <https://doi.org/10.1186/s12967-022-03231-y>.
- [39] S. Ju, C. Chen, J. Zhang, L. Xu, X. Zhang, Z. Li, Y. Chen, J. Zhou, F. Ji, L. Wang, Detection of circulating tumor cells: opportunities and challenges, *Biomark. Res.* 10 (2022) 58, <https://doi.org/10.1186/s40364-022-00403-2>.
- [40] Y.H. Soung, S. Ford, V. Zhang, J. Chung, Exosomes in cancer diagnostics, *Cancers* 9 (2017) 8, <https://doi.org/10.3390/cancers9010008>.
- [41] S. Tang, J. Cheng, Y. Yao, C. Lou, L. Wang, X. Huang, Y. Zhang, Combination of four serum exosomal miRNAs as novel diagnostic biomarkers for early-stage gastric cancer, *Front. Genet.* 11 (2020) 237, <https://doi.org/10.3389/fgene.2020.00237>.
- [42] H. Zhang, S. Xu, X. Liu, MicroRNA profiling of plasma exosomes from patients with ovarian cancer using high-throughput sequencing, *Oncol. Lett.* 17 (2019) 5601–5607, <https://doi.org/10.3892/ol.2019.10220>.
- [43] P. Zhang, X. Zhou, Y. Zeng, Multiplexed immunophenotyping of circulating exosomes on nano-engineered ExoProfile chip towards early diagnosis of cancer, *Chem. Sci.* 10 (2019) 5495–5504, <https://doi.org/10.1039/c9sc00961b>.
- [44] X. Wu, H. Zhao, A. Natalia, C.Z.J. Lim, N.R.Y. Ho, C.J. Ong, M.C.C. Teo, J.B.Y. So, H. Shao, Exosome-templated nanoplasmonics for multiparametric molecular profiling, *Sci. Adv.* 6 (2020), <https://doi.org/10.1126/sciadv.aba2556>.
- [45] X. Wang, X. Jiang, J. Li, J. Wang, H. Binang, S. Shi, W. Duan, Y. Zhao, Y. Zhang, Serum exosomal miR-1269a serves as a diagnostic marker and plays an oncogenic role in non-small cell lung cancer, *Thorac. Cancer* 11 (2020) 3436–3447, <https://doi.org/10.1111/1759-7714.13644>.
- [46] E. Castellanos-Rizaldos, D.G. Grimm, V. Tadigotla, J. Hurley, J. Healy, P.L. Neal, M. Sher, R. Venkatesan, C. Karlovich, M. Raponi, A. Krug, M. Noerholm, J. Tannous, B.A. Tannous, L.E. Raveh, J.K. Skog, Exosome-based detection of EGFR T790M in plasma from non-small cell lung cancer patients, *Clin. Cancer Res.* 24 (2018) 2944–2950, <https://doi.org/10.1158/1078-0432.Ccr-17-3369>.
- [47] S. Zhang, L. Du, L. Wang, X. Jiang, Y. Zhan, J. Li, K. Yan, W. Duan, Y. Zhao, L. Wang, Y. Wang, Y. Shi, C. Wang, Evaluation of serum exosomal lncRNA-based biomarker panel for diagnosis and recurrence prediction of bladder cancer, *J. Cell Mol. Med.* 23 (2019) 1396–1405, <https://doi.org/10.1111/jcmm.14042>.
- [48] Y. Zhan, L. Du, L. Wang, X. Jiang, S. Zhang, J. Li, K. Yan, W. Duan, Y. Zhao, L. Wang, Y. Wang, C. Wang, Expression signatures of exosomal long non-coding RNAs in urine serve as novel non-invasive biomarkers for diagnosis and recurrence prediction of bladder cancer, *Mol. Cancer* 17 (2018) 142, <https://doi.org/10.1186/s12943-018-0893-y>.

- [49] M. Li, X. Zou, T. Xia, T. Wang, P. Liu, X. Zhou, S. Wang, W. Zhu, A five-miRNA panel in plasma was identified for breast cancer diagnosis, *Cancer Med.* 8 (2019) 7006–7017, <https://doi.org/10.1002/cam4.2572>.
- [50] H. Wu, Q. Wang, H. Zhong, L. Li, Q. Zhang, Q. Huang, Z. Yu, Differentially expressed microRNAs in exosomes of patients with breast cancer revealed by next-generation sequencing, *Oncol. Rep.* 43 (2020) 240–250, <https://doi.org/10.3892/or.2019.7401>.
- [51] F.G. Ortega, S.V. Piguille, G.A. Messina, G.R. Tortella, O. Rubilar, M.I. Jiménez Castillo, J.A. Lorente, M.J. Serrano, J. Raba, M.A. Fernández Baldo, EGFR detection in extracellular vesicles of breast cancer patients through immunosensor based on silica-chitosan nanoplatfrom, *Talanta* 194 (2019) 243–252, <https://doi.org/10.1016/j.talanta.2018.10.016>.
- [52] F. Tian, S. Zhang, C. Liu, Z. Han, Y. Liu, J. Deng, Y. Li, X. Wu, L. Cai, L. Qin, Q. Chen, Y. Yuan, Y. Liu, Y. Cong, B. Ding, Z. Jiang, J. Sun, Protein analysis of extracellular vesicles to monitor and predict therapeutic response in metastatic breast cancer, *Nat. Commun.* 12 (2021) 2536, <https://doi.org/10.1038/s41467-021-22913-7>.
- [53] B. Li, C. Liu, W. Pan, J. Shen, J. Guo, T. Luo, J. Feng, B. Situ, T. An, Y. Zhang, L. Zheng, Facile fluorescent aptasensor using aggregation-induced emission luminogens for exosomal proteins profiling towards liquid biopsy, *Biosens. Bioelectron.* 168 (2020), 112520, <https://doi.org/10.1016/j.bios.2020.112520>.
- [54] B. Li, W. Pan, C. Liu, J. Guo, J. Shen, J. Feng, T. Luo, B. Situ, Y. Zhang, T. An, C. Xu, W. Zheng, L. Zheng, Homogenous magneto-fluorescent nanosensor for tumor-derived exosome isolation and analysis, *ACS Sens.* 5 (2020) 2052–2060, <https://doi.org/10.1021/acssens.0c00513>.
- [55] W. Liu, J. Li, Y. Wu, S. Xing, Y. Lai, G. Zhang, Target-induced proximity ligation triggers recombinase polymerase amplification and transcription-mediated amplification to detect tumor-derived exosomes in nasopharyngeal carcinoma with high sensitivity, *Biosens. Bioelectron.* 102 (2018) 204–210, <https://doi.org/10.1016/j.bios.2017.11.033>.
- [56] Y. Zhang, X. Zhang, B. Situ, Y. Wu, S. Luo, L. Zheng, Y. Qiu, Rapid electrochemical biosensor for sensitive profiling of exosomal microRNA based on multifunctional DNA tetrahedron assisted catalytic hairpin assembly, *Biosens. Bioelectron.* 183 (2021), 113205, <https://doi.org/10.1016/j.bios.2021.113205>.
- [57] J. Zhao, C. Liu, Y. Li, Y. Ma, J. Deng, L. Li, J. Sun, Thermophoretic detection of exosomal microRNAs by nanoflakes, *J. Am. Chem. Soc.* 142 (2020) 4996–5001, <https://doi.org/10.1021/jacs.9b13960>.
- [58] E.A. Kwizera, R. O'Connor, V. Vinduska, M. Williams, E.R. Butch, S.E. Snyder, X. Chen, X. Huang, Molecular detection and analysis of exosomes using surface-enhanced Raman scattering gold nanorods and a miniaturized device, *Theranostics* 8 (2018) 2722–2738, <https://doi.org/10.7150/thno.21358>.
- [59] Y. Li, J. Deng, Z. Han, C. Liu, F. Tian, R. Xu, D. Han, S. Zhang, J. Sun, Molecular identification of tumor-derived extracellular vesicles using thermophoresis-mediated DNA computation, *J. Am. Chem. Soc.* 143 (2021) 1290–1295, <https://doi.org/10.1021/jacs.0c12016>.
- [60] H. Zheng, J. Zhao, X. Wang, S. Yan, H. Chu, M. Gao, X. Zhang, Integrated pipeline of rapid isolation and analysis of human plasma exosomes for cancer discrimination based on deep learning of MALDI-TOF MS fingerprints, *Anal. Chem.* 94 (2022) 1831–1839, <https://doi.org/10.1021/acs.analchem.1c04762>.
- [61] J. Park, J.S. Park, C.H. Huang, A. Jo, K. Cook, R. Wang, H.Y. Lin, J. Van Deun, H. Li, J. Min, L. Wang, G. Yoon, B.S. Carter, L. Balaj, G.S. Choi, C.M. Castro, R. Weissleder, H. Lee, An integrated magneto-electrochemical device for the rapid profiling of tumour extracellular vesicles from blood plasma, *Nat. Biomed. Eng.* 5 (2021) 678–689, <https://doi.org/10.1038/s41551-021-00752-7>.
- [62] P. Wei, F. Wu, B. Kang, X. Sun, F. Heskia, A. Pachot, J. Liang, D. Li, Plasma extracellular vesicles detected by Single Molecule array technology as a liquid biopsy for colorectal cancer, *J. Extracell. Vesicles* 9 (2020), 1809765, <https://doi.org/10.1080/20013078.2020.1809765>.
- [63] L. Sun, X. Liu, B. Pan, X. Hu, Y. Zhu, Y. Su, Z. Guo, G. Zhang, M. Xu, X. Xu, H. Sun, S. Wang, Serum exosomal miR-122 as a potential diagnostic and prognostic biomarker of colorectal cancer with liver metastasis, *J. Cancer* 11 (2020) 630–637, <https://doi.org/10.7150/jca.33022>.
- [64] L. Zhou, W. Wang, F. Wang, S. Yang, J. Hu, B. Lu, Z. Pan, Y. Ma, M. Zheng, L. Zhou, S. Lei, P. Song, P. Liu, W. Lu, Y. Lu, Plasma-derived exosomal miR-15a-5p as a promising diagnostic biomarker for early detection of endometrial carcinoma, *Mol. Cancer* 20 (2021) 57, <https://doi.org/10.1186/s12943-021-01352-4>.
- [65] Y. Lin, H. Dong, W. Deng, W. Lin, K. Li, X. Xiong, Y. Guo, F. Zhou, C. Ma, Y. Chen, H. Ren, H. Yang, N. Dai, L. Ma, S.J. Meltzer, S.J. Yeung, H. Zhang, Evaluation of salivary exosomal chimeric GOLM1-NAA35 RNA as a potential biomarker in esophageal carcinoma, *Clin. Cancer Res.* 25 (2019) 3035–3045, <https://doi.org/10.1158/1078-0432.Ccr-18-3169>.
- [66] R. Zhao, Y. Zhang, X. Zhang, Y. Yang, X. Zheng, X. Li, Y. Liu, Y. Zhang, Exosomal long noncoding RNA HOTTIP as potential novel diagnostic and prognostic biomarker test for gastric cancer, *Mol. Cancer* 17 (2018) 68, <https://doi.org/10.1186/s12943-018-0817-x>.
- [67] S. Wei, L. Peng, J. Yang, H. Sang, D. Jin, X. Li, M. Chen, W. Zhang, Y. Dang, G. Zhang, Exosomal transfer of miR-15b-3p enhances tumorigenesis and malignant transformation through the DYNLT1/Caspase-3/Caspase-9 signaling pathway in gastric cancer, *J. Exp. Clin. Cancer Res.* 39 (2020) 32, <https://doi.org/10.1186/s13046-019-1511-6>.
- [68] Z. Yao, C. Jia, Y. Tai, H. Liang, Z. Zhong, Z. Xiong, M. Deng, Q. Zhang, Serum exosomal long noncoding RNAs Inc-FAM72D-3 and Inc-EPC1-4 as diagnostic biomarkers for hepatocellular carcinoma, *Aging* 12 (2020) 11843–11863, <https://doi.org/10.18632/aging.103355>.
- [69] X. Huang, L. Sun, S. Wen, D. Deng, F. Wan, X. He, L. Tian, L. Liang, C. Wei, K. Gao, Q. Fu, Y. Li, J. Jiang, R. Zhai, M. He, RNA sequencing of plasma exosomes revealed novel functional long noncoding RNAs in hepatocellular carcinoma, *Cancer Sci.* 111 (2020) 3338–3349, <https://doi.org/10.1111/cas.14516>.
- [70] Y. Cui, H.F. Xu, M.Y. Liu, Y.J. Xu, J.C. He, Y. Zhou, S.D. Cang, Mechanism of exosomal microRNA-224 in development of hepatocellular carcinoma and its diagnostic and prognostic value, *World J. Gastroenterol.* 25 (2019) 1890–1898, <https://doi.org/10.3748/wjg.v25.i15.1890>.
- [71] H.J. Cho, J.W. Eun, G.O. Baek, C.W. Seo, H.R. Ahn, S.S. Kim, S.W. Cho, J.Y. Cheong, Serum exosomal microRNA, miR-10b-5p, as a potential diagnostic biomarker for early-stage hepatocellular carcinoma, *J. Clin. Med.* 9 (2020), <https://doi.org/10.3390/jcm9010281>.
- [72] Y. Wang, C. Zhang, P. Zhang, G. Guo, T. Jiang, X. Zhao, J. Jiang, X. Huang, H. Tong, Y. Tian, Serum exosomal microRNAs combined with alpha-fetoprotein as diagnostic markers of hepatocellular carcinoma, *Cancer Med.* 7 (2018) 1670–1679, <https://doi.org/10.1002/cam4.1390>.
- [73] C. Liu, J. Zhao, F. Tian, L. Cai, W. Zhang, Q. Feng, J. Chang, F. Wan, Y. Yang, B. Dai, Y. Cong, B. Ding, J. Sun, W. Tan, Low-cost thermophoretic profiling of extracellular-vesicle surface proteins for the early detection and classification of cancers, *Nat. Biomed. Eng.* 3 (2019) 183–193, <https://doi.org/10.1038/s41551-018-0343-6>.
- [74] D. Jin, X.X. Peng, Y. Qin, P. Wu, H. Lu, L. Wang, J. Huang, Y. Li, Y. Zhang, G.J. Zhang, F. Yang, Multivalence-actuated DNA nanomachines enable bicolor exosomal phenotyping and PD-L1-guided therapy monitoring, *Anal. Chem.* 92 (2020) 9877–9886, <https://doi.org/10.1021/acs.analchem.0c01387>.
- [75] H. Wang, D. Jiang, W. Li, X. Xiang, J. Zhao, B. Yu, C. Wang, Z. He, L. Zhu, Y. Yang, Evaluation of serum extracellular vesicles as noninvasive diagnostic markers of glioma, *Theranostics* 9 (2019) 5347–5358, <https://doi.org/10.7150/thno.33114>.
- [76] M. Stella, L. Falzone, A. Caponnetto, G. Gattuso, C. Barbagallo, R. Battaglia, F. Mirabella, G. Broggi, R. Altieri, F. Certo, R. Caltabiano, G.M.V. Barbagallo, P. Musumeci, M. Ragusa, C.D. Pietro, M. Libra, M. Purrello, D. Barbagallo, Serum extracellular vesicle-derived circHIPK3 and circSMARCA5 are two novel diagnostic biomarkers for glioblastoma multiforme, *Pharmaceuticals* 14 (2021) 618, <https://doi.org/10.3390/ph14070618>.
- [77] N. Sun, Y.T. Lee, R.Y. Zhang, R. Kao, P.C. Teng, Y. Yang, P. Yang, J.J. Wang, M. Smalley, P.J. Chen, M. Kim, S.J. Chou, L. Bao, J. Wang, X. Zhang, D. Qi, J. Palomique, N. Nissen, S.B. Han, S. Sadeghi, R.S. Finn, S. Saab, R.W. Busuttill, D. Markovic, D. Elashoff, H.H. Yu, H. Li, A.P. Heaney, E. Posadas, S. You, J.D. Yang, R. Pei, V.G. Agopian, H.R. Tseng, Y. Zhu, Purification of HCC-specific extracellular vesicles on nanosubstrates for early HCC detection by digital scoring, *Nat. Commun.* 11 (2020) 4489, <https://doi.org/10.1038/s41467-020-18311-0>.
- [78] T. Nakano, I.H. Chen, C.C. Wang, P.J. Chen, H.P. Tseng, K.T. Huang, T.H. Hu, L.C. Li, S. Goto, Y.F. Cheng, C.C. Lin, C.L. Chen, Circulating exosomal miR-92b: its role for cancer immunoediting and clinical value for prediction of posttransplant hepatocellular carcinoma recurrence, *Am. J. Transplant.* 19 (2019) 3250–3262, <https://doi.org/10.1111/ajt.15490>.
- [79] Z. Ramshani, C. Zhang, K. Richards, L. Chen, G. Xu, B.L. Stiles, R. Hill, S. Senapati, D.B. Go, H.C. Chang, Extracellular vesicle microRNA quantification from plasma using an integrated microfluidic device, *Commun. Biol.* 2 (2019) 189, <https://doi.org/10.1038/s42003-019-0435-1>.
- [80] H. Shin, S. Oh, S. Hong, M. Kang, D. Kang, Y.G. Ji, B.H. Choi, K.W. Kang, H. Jeong, Y. Park, S. Hong, H.K. Kim, Y. Choi, Early-stage lung cancer diagnosis by deep learning-based spectroscopic analysis of circulating exosomes, *ACS Nano* 14 (2020) 5435–5444, <https://doi.org/10.1021/acsnano.9b09119>.
- [81] Y. Bai, Y. Qu, Z. Wu, Y. Ren, Z. Cheng, Y. Lu, J. Hu, J. Lou, J. Zhao, C. Chen, H. Mao, Absolute quantification and analysis of extracellular vesicle lncRNAs from the peripheral blood of patients with lung cancer based on multi-colour fluorescence chip-based digital PCR, *Biosens. Bioelectron.* 142 (2019), 111523, <https://doi.org/10.1016/j.bios.2019.111523>.
- [82] D. Zocco, S. Bernardi, M. Novelli, C. Astrua, P. Fava, N. Zarovni, F.M. Carpi, L. Bianciardi, O. Malavenda, P. Quaglino, C. Foroni, D. Russo, A. Chiesi, M.T. Fierro, Isolation of extracellular vesicles improves the detection of mutant DNA from plasma of metastatic melanoma patients, *Sci. Rep.* 10 (2020), 15745, <https://doi.org/10.1038/s41598-020-72834-6>.
- [83] S. Xing, Z. Lu, Q. Huang, H. Li, Y. Wang, Y. Lai, Y. He, M. Deng, W. Liu, An ultrasensitive hybridization chain reaction-amplified CRISPR-Cas12a aptasensor for extracellular vesicle surface protein quantification, *Theranostics* 10 (2020) 10262–10273, <https://doi.org/10.7150/thno.49047>.
- [84] H. Li, S. Xing, J. Xu, Y. He, Y. Lai, Y. Wang, G. Zhang, S. Guo, M. Deng, M. Zeng, W. Liu, Aptamer-based CRISPR/Cas12a assay for the ultrasensitive detection of extracellular vesicle proteins, *Talanta* 221 (2021), 121670, <https://doi.org/10.1016/j.talanta.2020.121670>.
- [85] Y. Pang, J. Shi, X. Yang, C. Wang, Z. Sun, R. Xiao, Personalized detection of circling exosomal PD-L1 based on Fe₃O₄@TiO₂ isolation and SERS immunoassay, *Biosens. Bioelectron.* 148 (2020), 111800, <https://doi.org/10.1016/j.bios.2019.111800>.
- [86] P. Zhang, X. Zhou, M. He, Y. Shang, A.L. Tetlow, A.K. Godwin, Y. Zeng, Ultrasensitive detection of circulating exosomes with a 3D-nanopatterned microfluidic chip, *Nat. Biomed. Eng.* 3 (2019) 438–451, <https://doi.org/10.1038/s41551-019-0356-9>.
- [87] Y.Y. Su, L. Sun, Z.R. Guo, J.C. Li, T.T. Bai, X.X. Cai, W.H. Li, Y.F. Zhu, Upregulated expression of serum exosomal miR-375 and miR-1307 enhance the diagnostic power of CA125 for ovarian cancer, *J. Ovarian Res.* 12 (2019) 6, <https://doi.org/10.1186/s13048-018-0477-x>.
- [88] J. Liu, J. Yoo, J.Y. Ho, Y. Jung, S. Lee, S.Y. Hur, Y.J. Choi, Plasma-derived exosomal miR-4732-5p is a promising noninvasive diagnostic biomarker for epithelial ovarian cancer, *J. Ovarian Res.* 14 (2021) 59, <https://doi.org/10.1186/s13048-021-00814-z>.

- [89] J. Yang, B. Pan, F. Zeng, B. He, Y. Gao, X. Liu, Y. Song, Magnetic colloid antibodies accelerate small extracellular vesicles isolation for point-of-care diagnostics, *Nano Lett.* 21 (2021) 2001–2009, <https://doi.org/10.1021/acs.nanolett.0c04476>.
- [90] S. Kim, M.C. Choi, J.Y. Jeong, S. Hwang, S.G. Jung, W.D. Joo, H. Park, S.H. Song, C. Lee, T.H. Kim, H.J. An, Serum exosomal miRNA-145 and miRNA-200c as promising biomarkers for preoperative diagnosis of ovarian carcinomas, *J. Cancer* 10 (2019) 1958–1967, <https://doi.org/10.7150/jca.30231>.
- [91] S. Jiang, Q. Li, C. Wang, Y. Pang, Z. Sun, R. Xiao, In situ exosomal microRNA determination by target-triggered SERS and Fe₃O₄@TiO₂-based exosome accumulation, *ACS Sens.* 6 (2021) 852–862, <https://doi.org/10.1021/acssensors.0c01900>.
- [92] M. Rodrigues, N. Richards, B. Ning, C.J. Lyon, T.Y. Hu, Rapid lipid-based approach for normalization of quantum-dot-detected biomarker expression on extracellular vesicles in complex biological samples, *Nano Lett.* 19 (2019) 7623–7631, <https://doi.org/10.1021/acs.nanolett.9b02232>.
- [93] J.M. Lewis, A.D. Vyas, Y. Qiu, K.S. Messer, R. White, M.J. Heller, Integrated analysis of exosomal protein biomarkers on alternating current electrokinetic chips enables rapid detection of pancreatic cancer in patient blood, *ACS Nano* 12 (2018) 3311–3320, <https://doi.org/10.1021/acsnano.7b08199>.
- [94] T.D. Li, R. Zhang, H. Chen, Z.P. Huang, X. Ye, H. Wang, A.M. Deng, J.L. Kong, An ultrasensitive polydopamine bi-functionalized SERS immunoassay for exosome-based diagnosis and classification of pancreatic cancer, *Chem. Sci.* 9 (2018) 5372–5382, <https://doi.org/10.1039/c8sc01611a>.
- [95] S. Li, Y. Zhao, W. Chen, L. Yin, J. Zhu, H. Zhang, C. Cai, P. Li, L. Huang, P. Ma, Exosomal ephrinA2 derived from serum as a potential biomarker for prostate cancer, *J. Cancer* 9 (2018) 2659–2665, <https://doi.org/10.7150/jca.25201>.
- [96] T. Liyanage, B. Alharbi, L. Quan, A. Esquela-Kerscher, G. Slaughter, Plasmonic-based biosensor for the early diagnosis of prostate cancer, *ACS Omega* 7 (2022) 2411–2418, <https://doi.org/10.1021/acsomega.1c06479>.
- [97] D. Bhagirath, T.L. Yang, N. Bucay, K. Sekhon, S. Majid, V. Shahyari, R. Dahiya, Y. Tanaka, S. Saini, MicroRNA-1246 is an exosomal biomarker for aggressive prostate cancer, *Cancer Res.* 78 (2018) 1833–1844, <https://doi.org/10.1158/0008-5472.Can-17-2069>.
- [98] J. Deng, S. Zhao, J. Li, Y. Cheng, C. Liu, Z. Liu, L. Li, F. Tian, B. Dai, J. Sun, One-step thermophoretic AND gate operation on extracellular vesicles improves diagnosis of prostate cancer, *Angew. Chem., Int. Ed. Engl.* 61 (2022), e202207037, <https://doi.org/10.1002/anie.202207037>.
- [99] K. Xu, Y. Jin, Y. Li, Y. Huang, R. Zhao, Recent progress of exosome isolation and peptide recognition-guided strategies for exosome research, *Front. Chem.* 10 (2022), 844124, <https://doi.org/10.3389/fchem.2022.844124>.
- [100] SBI System biosciences, ExoQuick® ULTRA EV Isolation Kit for Serum and Plasma Cat # EQULTRA-20A-1 User Manual, 2018. https://www.systembio.com/wp-content/uploads/2020/10/MANUAL_ExoQuick-ULTRA_Serum_Plasma_V3.pdf. (Accessed 13 April 2022). accessed.
- [101] F.S. Ligler, J.J. Gooding, Lighting up biosensors: now and the decade to come, *Anal. Chem.* 91 (2019) 8732–8738, <https://doi.org/10.1021/acs.analchem.9b00793>.
- [102] H. Shao, H. Im, C.M. Castro, X. Breakefield, R. Weissleder, H. Lee, New technologies for analysis of extracellular vesicles, *Chem. Rev.* 118 (2018) 1917–1950, <https://doi.org/10.1021/acs.chemrev.7b00534>.
- [103] H. Xu, C. Liao, P. Zuo, Z. Liu, B.C. Ye, Magnetic-based microfluidic device for on-chip isolation and detection of tumor-derived exosomes, *Anal. Chem.* 90 (2018) 13451–13458, <https://doi.org/10.1021/acs.analchem.8b03272>.
- [104] Y. Fan, X. Wang, J. Ren, F. Lin, J. Wu, Recent advances in acoustofluidic separation technology in biology, *Microsyst. Nanoeng.* 8 (2022) 94, <https://doi.org/10.1038/s41378-022-00435-6>.
- [105] K. Lee, H. Shao, R. Weissleder, H. Lee, Acoustic purification of extracellular microvesicles, *ACS Nano* 9 (2015) 2321–2327, <https://doi.org/10.1021/nn506538f>.
- [106] M. Wu, Y. Ouyang, Z. Wang, R. Zhang, P.H. Huang, C. Chen, H. Li, P. Li, D. Quinn, M. Dao, S. Suresh, Y. Sadovsky, T.J. Huang, Isolation of exosomes from whole blood by integrating acoustics and microfluidics, *Proc. Natl. Acad. Sci. U. S. A.* 114 (2017) 10584–10589, <https://doi.org/10.1073/pnas.1709210114>.
- [107] Z. Wang, F. Li, J. Rufo, C. Chen, S. Yang, L. Li, J. Zhang, J. Cheng, Y. Kim, M. Wu, E. Abemayor, M. Tu, D. Chia, R. Spruce, N. Batis, H. Mehanna, D.T.W. Wong, T.J. Huang, Acoustofluidic salivary exosome isolation: a liquid biopsy compatible approach for human papillomavirus-associated oropharyngeal cancer detection, *J. Mol. Diagn.* 22 (2020) 50–59, <https://doi.org/10.1016/j.jmoldx.2019.08.004>.
- [108] Y. Chen, Q. Zhu, L. Cheng, Y. Wang, M. Li, Q. Yang, L. Hu, D. Lou, J. Li, X. Dong, L.P. Lee, F. Liu, Exosome detection via the ultrafast-isolation system: exodus, *Nat. Methods* 18 (2021) 212–218, <https://doi.org/10.1038/s41592-020-01034-x>.
- [109] A.K. Krug, D. Enderle, C. Karlovich, T. Priewasser, S. Bentink, A. Spiel, K. Brinkmann, J. Emenegger, D.G. Grimm, E. Castellanos-Rizaldos, J.W. Goldman, L.V. Sequist, J.C. Soria, D.R. Camidge, S.M. Gadgeel, H.A. Wakelee, M. Raponi, M. Noerholm, J. Skog, Improved EGFR mutation detection using combined exosomal RNA and circulating tumor DNA in NSCLC patient plasma, *Ann. Oncol.* 29 (2018) 700–706, <https://doi.org/10.1093/annonc/mdx765>.
- [110] M. Notarangelo, C. Zucal, A. Modelska, I. Pesce, G. Scardueli, C. Potrich, L. Lunelli, C. Pederzoli, P. Pavan, G. la Marca, L. Pasini, P. Ulivi, H. Beltran, F. Demicheli, A. Provenzani, A. Quattrone, V.G. D'Agostino, Ultrasensitive detection of cancer biomarkers by nickel-based isolation of polydisperse extracellular vesicles from blood, *EBioMedicine* 43 (2019) 114–126, <https://doi.org/10.1016/j.ebiom.2019.04.039>.
- [111] S. Sun, H. Chen, C. Xu, Y. Zhang, Q. Zhang, L. Chen, Q. Ding, Z. Deng, Exosomal miR-106b serves as a novel marker for lung cancer and promotes cancer metastasis via targeting PTEN, *Life Sci.* 244 (2020), 117297, <https://doi.org/10.1016/j.lfs.2020.117297>.
- [112] Y. Liang, B.M. Lehrich, S. Zheng, M. Lu, Emerging methods in biomarker identification for extracellular vesicle-based liquid biopsy, *J. Extracell. Vesicles* 10 (2021), e12090, <https://doi.org/10.1002/jev.212090>.
- [113] S. Kasetsirikul, K.T. Tran, K. Clack, N. Soda, M.J.A. Shiddiky, N.T. Nguyen, Low-cost electrochemical paper-based device for exosome detection, *Analyst* 147 (2022) 3732–3740, <https://doi.org/10.1039/d2an00875k>.
- [114] D. Pan, Y. Lin, X. Liu, Y. Xin, Q. Tian, J. Zhang, Ultrasensitive and preprocessing-free electrochemical biosensing platform for the detection of cancer-derived exosomes based on spiky-shaped aptamer-magnetic beads, *Biosens. Bioelectron.* 217 (2022), 114705, <https://doi.org/10.1016/j.bios.2022.114705>.
- [115] W. Chen, Z. Li, W. Cheng, T. Wu, J. Li, X. Li, L. Liu, H. Bai, S. Ding, X. Li, X. Yu, Surface plasmon resonance biosensor for exosome detection based on reformative tyramine signal amplification activated by molecular aptamer beacon, *J. Nanobiotechnol.* 19 (2021) 450, <https://doi.org/10.1186/s12951-021-01210-x>.
- [116] J. Zhang, Y. Zhu, M. Guan, Y. Liu, M. Lv, C. Zhang, H. Zhang, Z. Zhang, Isolation of circulating exosomes and identification of exosomal PD-L1 for predicting immunotherapy response, *Nanoscale* 14 (2022) 8995–9003, <https://doi.org/10.1039/d2nr00829g>.
- [117] Y. Xie, X. Su, Y. Wen, C. Zheng, M. Li, Artificial intelligent label-free SERS profiling of serum exosomes for breast cancer diagnosis and postoperative assessment, *Nano Lett.* 22 (2022) 7910–7918, <https://doi.org/10.1021/acs.nanolett.2c02928>.
- [118] Y. Zhu, H. Pick, N. Gasilova, X. Li, T.E. Lin, H.P. Laeubli, A. Zippelius, P.C. Ho, H.H. Girault, MALDI detection of exosomes: a potential tool for cancer studies, *Chem* 5 (2019) 1318–1336, <https://doi.org/10.1016/j.chempr.2019.04.007>.
- [119] Z. Han, J. Yi, Y. Yang, D. Li, C. Peng, S. Long, X. Peng, Y. Shen, B. Liu, L. Qiao, SERS and MALDI-TOF MS based plasma exosome profiling for rapid detection of osteosarcoma, *Analyst* 146 (2021) 6496–6505, <https://doi.org/10.1039/d1an01163d>.
- [120] X. Sun, L. Huang, R. Zhang, W. Xu, J. Huang, D.D. Gurav, V. Vedarethinam, R. Chen, J. Lou, Q. Wang, J. Wan, K. Qian, Metabolic fingerprinting on a plasmonic gold chip for mass spectrometry based *in vitro* diagnostics, *ACS Cent. Sci.* 4 (2018) 223–229, <https://doi.org/10.1021/acscentsci.7b00546>.
- [121] S. Sharma, J. Zapatero-Rodríguez, P. Estrela, R. O'Kennedy, Point-of-care diagnostics in low resource settings: present status and future role of microfluidics, *Biosensors* 5 (2015) 577–601, <https://doi.org/10.3390/bios5030577>.
- [122] E.M. Burd, Validation of laboratory-developed molecular assays for infectious diseases, *Clin. Microbiol. Rev.* 23 (2010) 550–576, <https://doi.org/10.1128/cmr.00074-09>.
- [123] The Pew Charitable Trusts, The Role of Lab-Developed Tests in the *In Vitro* Diagnostics Market as Lab-Developed Tests Grow Increasingly Complicated, Federal Oversight Has Lagged, 2021. <https://www.pewtrusts.org/-/media/assets/2021/10/understanding-the-role-of-lab-developed-tests-in-vitro-diagnostics.pdf>. (Accessed 10 July 2022). accessed.
- [124] K.W. Witwer, E.I. Buzás, L.T. Bemis, A. Bora, C. Lässer, J. Lötvall, E.N. Nolte-t Hoen, M.G. Piper, S. Sivaraman, J. Skog, C. Théry, M.H. Wauben, F. Hochberg, Standardization of sample collection, isolation and analysis methods in extracellular vesicle research, *J. Extracell. Vesicles* 2 (2013), <https://doi.org/10.3402/jev.v2i0.20360>.
- [125] R. Tutrone, M.J. Donovan, P. Torkler, V. Tadigotla, T. McLain, M. Noerholm, J. Skog, J. McKiernan, Clinical utility of the exosome based ExoDx Prostate(IntelliScore) EPI test in men presenting for initial Biopsy with a PSA 2–10 ng/mL, *Prostate Cancer Prostatic Dis.* 23 (2020) 607–614, <https://doi.org/10.1038/s41391-020-0237-z>.